



**Anticancer activity of CT-p19LC, a synthetic peptide
derived from the bacterial protein azurin**

Lígia Patrícia Fonseca Coelho

Thesis to obtain the Master of Science Degree in
Microbiology

Supervisor: Prof. Arsénio do Carmo Sales Mendes Fialho

Co-supervisor: Dr. Nuno Filipe Santos Bernardes

Examination Committee

Chairperson: Prof. Isabel Maria De Sá Correia Leite de Almeida (DBE)

Supervisor: Prof. Arsénio Do Carmo Sales Mendes Fialho (DBE)

Member of the Committee: Prof. Leonilde De Fátima Morais Moreira (DBE)

September, 2017

“The human body is strange and flawed and unpredictable. The human body has many secrets, and it does not divulge them to anyone, except those who have learned to wait.”

Paul Auster in Sunset Park

Acknowledgments

First, I would like to express my immense gratitude toward my supervisors: Professor Arsénio Fialho and Dr. Nuno Bernardes for all the guidance, firmness and tremendous patience, which allowed my development as a person, student and hopefully as a scientist. I will most certainly remember all your advices and seek to use what you taught me in the future.

My gratefulness goes also to the BSRG members for making me feel part of the team and helping me whenever I needed, especially Dr. Dalila Mil-Homens and Mónica Rato. I would like to thank Dr. Sandra Pinto for the support with the confocal microscopy and advices about the work.

In addition, with immense appreciation I would like to thank my lab peers Ana Rita Garizo, Andreia Almeida, Marcelo Ramirez, Marília Silva, Rui Martins and Soraia Guerreiro for always making it possible to count on them, for the complicity and friendship.

I wish to take this opportunity to thank my family, especially my mother Luisa Fonseca for all unconditional support and for having confidence in me. To my brother, Fernando Coelho, for always being there to listen and to my boyfriend, Frederico Martins, for all the patience during the long hours away in the course of this master and the support through the most difficult times. I also thank all my friends in and outside Técnico for the good moments which made the bad ones bearable.

During my masters in IST I also counted with the guidance of some very dedicated professors and investigators and to them I also send my sincere thank you.

Last, but not least, I would like to thank Microbiology master's coordinator professor Isabel Sá-Correia.

Funding received by iBB-Institute for Bioengineering and Biosciences from FCT (UID/BIO/04565/2013) and from Programa Operacional Regional de Lisboa 2020 (Project N.007317) is acknowledged (iBB/2015/12 and IBB/2015/16).

Abstract

Several cationic peptides have recently been shown to display anticancer activity through a mechanism that usually requires the disruption of cancer cell membranes. In this thesis project, we designed a 19-residue presumptive ACP_{AO}, designated CT-p19LC, using as template CT-p26, a 26-residue peptide derived from the protein azurin. Produced by *Pseudomonas aeruginosa*, the bacteriocin azurin has been explored regarding its multi-target anticancer potential. Accordingly, one domain of azurin comprising 28 amino acids (p28) has already passed two phase I US clinical trials showing promise potential against solid tumors and being considered safe for humans. However, it was demonstrated in previous studies that azurin deleterious effect at the membrane level of epithelial cancer cell lines is closely related to a phenylalanine residue in position 114 near its C-terminal. Thus, CT-p26, a peptide which comprises the azurin region from 94-120 amino acids was tested against breast and lung cancer cell lines demonstrating a significant cytotoxic effect. In the present study we took advantage of appropriate bioinformatics peptide optimization tools and performed an *in silico* analysis with the objective of improving the anticancer activity and reducing the length of CT-p26. This analysis originated CT-p19LC, a shorter peptide with point residue alterations with higher hydrophobicity, positive net charge and improved solubility. Consequently, *in vitro* MTT cell proliferation assays proved CT-p19LC is active against lung (A549), breast (MCF-7), colorectal (HT-29) and cervix (HeLa) adenocarcinoma cell lines treated in different doses whereas the cytotoxicity toward noncancerous cells such as breast (MCF-10A) and lung (16HBE14) is low. Promising results suggest that not only CT-p19LC is more active against breast (MCF-7) and (A549) when compared with results from CT-p26 or even p28 but also that LD₅₀ was less than half of reference dose concentration. Membrane order assay with Laurdan's probe along with confocal microscopy gave quantification data which may support the intended mechanism of action at the cell's membrane level, although alternatives are also discussed. Finally, CT-p19LC appears to enhance erlotinib anticancer action in A549 lung cancer cells. This small chemical inhibitor drug acts at the membrane receptor EGFR, a protein complex of interest in cancer invasion and drug resistance. Consequently, this work shows that levels of EGFR are disturbed by the treatment of CT-p19LC which may represent the first clue of the cell target of this newly design peptide and be the foundation for future studies.

Key words: Anticancer peptide, azurin, peptide-based drug development, *in silico*, chemotherapeutics, drug resistance

Resumo

Recentemente, vários péptidos catiónicos têm demonstrado actividade anticancerígena por um mecanismo que normalmente induz a ruptura das membranas celulares. Neste projecto de tese, foi desenhado um péptido presumivelmente ACP_{AO} com 19 resíduos, designado de CT-p19LC, utilizando como molde o CT-p26, um péptido de 26 resíduos derivado da proteína azurina. Produzida por *Pseudomonas aeruginosa*, a bacteriocina azurina tem sido estudada quanto ao seu potencial anticancerígeno com multi-alvos. O péptido p28, derivado da azurina, completou já dois ensaios clínicos de fase I mostrando potencial contra tumores sólidos e apresentando-se como seguro para humanos. Já foi demonstrado em ensaios prévios que o efeito citotóxico a nível membranar da azurina contra linhas celulares de tecido epithelial cancerígeno está relacionado com outro dos seus domínios que compreendem o resíduo fenilalanina na posição 114 da extremidade C-terminal. Assim, o péptido CT-p26, que compreende a região da azurina entre os aminoácidos 94-112 foi testado contra linhas celulares cancerígenas da mama e do pulmão demonstrando um potencial citotóxico significativo. No presente estudo, utilizámos as ferramentas bioinformáticas apropriadas de optimização de péptidos para efectuar um estudo *in silico* com o objectivo de melhorar o potencial anticancerígeno e reduzir o tamanho do péptido CT-p26. Esta análise originou o CT-p19LC, um péptido com menos aminoácidos e com alterações em três destes resíduos que resultou num maior poder hidrofóbico, carga catiónica e melhor solubilidade que o seu molde. Ensaio *in vitro* de proliferação celular (MTT) provaram que CT-p19LC é activo contra células de adenocarcinoma do pulmão (A549), da mama (MCF-7), do cólon (HT-29) e do colo do útero (HeLa) tratadas com diferentes doses. No entanto, a citotoxicidade observada em células não malignas, tal como células da mama (MCF-10A) e do pulmão (16HBE14), é baixa. Resultados promissores sugerem que não só o CT-p19LC é mais activo contra células de cancro da mama (MCF-7) e do pulmão (A549) em comparação com o CT-p26 ou até mesmo o p28 bem como o LD₅₀ é inferior em mais de metade em comparação com os valores de referência. Ensaio de ordem membranar com a sonda de Laurdan e auxílio do microscópio confocal transmitiram dados quantitativos que suportam o mecanismo de acção pretendido para este péptido a nível da membrana. Por fim, o CT-p19LC parece ter um efeito estimulante na actividade do erlotinib contra células de cancro do pulmão (A549). Este fármaco actua a nível da membrana tendo como alvo o EGFR, uma proteína membranar de interesse na invasão deste cancro e na sua capacidade de resistir a fármacos. Este trabalho mostra que os níveis de EGFR das células A549 são perturbados pelo tratamento de CT-p19LC o que pode representar a primeira pista do alvo celular deste novo péptido e ser a base para futuros estudos.

Palavras-chave: Péptido anticancerígeno, azurina, desenvolvimento de fármacos baseados em péptidos, *in silico*, quimioterápicos, resistência a fármacos

Table of Contents

Acknowledgments	iii
Abstract	iv
Resumo	v
Index of figures	viii
Index of tables	xi
List of abbreviations	xii
1. Introduction	1
1.1. Anticancer and antimicrobial peptides	2
1.2. ACPs as a selective oncolytic therapy	3
1.3. Bioactivity of ACP's against cancer cells	7
1.3.1. Membranolytic effect based on electrostatic interactions	7
1.3.2. Other molecular targets	11
1.4. <i>In silico</i> drug design of new anticancer peptides	13
1.5. Peptides tailored from azurin	14
1.5.1. p28, a success case in early clinical trials	16
1.5.2. CT-p26 is active against epithelial tumor cell lines	17
1.5.3. Lipid rafts' components and potential therapeutic targets	18
2. Objectives and thesis outline	19
3. Materials and methods	20
3.1. <i>In silico</i> analysis	20
3.2. Peptides	20
3.3. Cell culture	20
3.4. MTT cell proliferation assay	21
3.5. Two-photon excitation microscopy – GP determination	21
3.6. Antibodies	22
3.7. Protein extraction and Western blot	22
3.8. Statistical analysis	23
4. Results and discussion	24

4.1.	Cytotoxic effect of azurin and derived peptides on cancer cells	24
4.2.	<i>In silico</i> optimization of CT-p26	25
4.2.1.	Computational study of CT-p26.....	25
4.2.2.	Improvement of CT-p26.....	28
4.3.	Cytotoxic effect of newly designed CT-p19LC on cancer cells	31
4.4.	CT-p19LC is not effective against breast and lung non-cancer cell lines	35
4.5.	CT-p19LC decreases the membrane order of cancer cell lines.....	36
4.6.	Treatment with CT-p19LC in combination with erlotinib potentiates the anticancer effect of this agent in lung cancer cell line A549	41
4.7.	CT-p19LC perturbs EGF-stimulated trigger of phosphorylated EGFR (Y1068) on A549 lung cancer cells	43
5.	Conclusions and future perspectives in cancer therapy.....	45
6.	References	48
	Appendix	a

Index of figures

Figure 1| Anticancer peptides (ACPs) modes of action may include disruption of plasma/ mitochondrial membranes, necrosis and apoptosis. **Membranolytic effect:** The peptide targets the membrane components and attach. This interaction creates pores or completely disrupts the membrane (Gaspar et al. 2013). **Apoptosis:** The mitochondrial membrane can also suffer the lytic effect of these peptides resulting on the releasing of cytochrome C (CytC) which will be available to bind to caspase-9. This complex triggers the apoptotic intrinsic signaling cascade (Yang et al. 2008). **Membrane receptors:** ACPs bind to natural membrane receptors taking advantage of their natural chemical binding to interact with cancer cells membrane (Leuschner 2005). **Anti-angiogenesis:** ACPs inhibit angiogenesis factors preventing cancer cells from tissue invasion. **DNA synthesis inhibition:** during DNA replication, some ACPs have the ability of interlacing with the newly synthesized chain obstructing the whole mechanism (Ourth 2011). **Mediated immunity:** dendritic cells are activated and directed to cancer cells by the action of some ACPs (Y. S. Wang et al. 2009). 10

Figure 2| Schematic representation of the primary sequence of azurin and its derived peptides (p28 and CT-p26). Following, graphic representation of the cytotoxic effect of azurin and the peptides in lung cancer cell line (A549) and breast cancer cell line (MCF-7) at a concentration of 100 μ M. 24

Figure 3| Linear molecular structure of CT-p19LC..... 29

Figure 4| Representation of the effect of CT-p19LC on A549 (lung adenocarcinoma), MCF-7 (breast adenocarcinoma), HT-29 (colorectal adenocarcinoma), and HeLa (cervix adenocarcinoma) cells. These results were obtained by multiple MTT proliferation assays, on each assay every condition was triplicate. The tested concentrations were between the control 0 μ M (untreated) and 100 μ M. Results were compared to the untreated condition by analysis of variance ANOVA (Newman-Keuls Multiple Comparisons, using GraphPad Prism ver 6). Values of $p < 0.05$ were considered statistically significant (*: $p < 0.05$). 31

Figure 5| Schematic representation of the primary sequence of azurin and its derived peptides (p28, CT-p26, CT-p19 and CT-p19LC). Following, graphic representation of the cytotoxic effect of Azurin and the peptides in lung cancer cell line (A549) and breast cancer cell line (MCF-7) at their most lethal concentrations. Results were compared by analysis of variance ANOVA (Newman-Keuls Multiple Comparisons, using GraphPad Prism ver 6). Values of $p < 0.05$ were considered statistically significant (*: $p < 0.05$). 33

Figure 6| Cytotoxic effect of azurin derived CT-p19LC on human bronchial epithelial (16HBE14) cell line and human breast (MCF-10A) cell line. Viability decrease refers to cell death after 48h MTT assay where cells were treated one time with the respective peptide in the represented doses, each condition triplicate. 35

Figure 7| Impact of CT-p19 on the membrane fluidity of cancer cell lines MCF-7, A549, HeLa and HT-29. Cells were loaded with 5 μM of Laurdan after incubation with 20 μM of peptide for 2 hours. Laurdan GP values were determined as described in Material and Methods..... 37

Figure 8| The effects of CT-p19LC in the cell's membrane order of A549 lung cancer cell line, MCF-7 breast cancer cell line, HT-29 colorectal cancer cell line and HeLa cervix cell line and their respective GP values. All represented cell lines were seeded on μ -Slide glass 8 well glass bottom chambers and treated with 20 μM of CT-p19LC for 2h. For each condition 5 μM of Laurdan were used. Untreated cells were the control. Software based on a MATLAB environment was used to measure the GP values. Average GP values are expressed as mean \pm SD from at least 15 individual cells in each condition. Results were compared to the untreated by student's t-test two tailed distribution two sample equal variance (****: $p < 0,0001$)..... 38

Figure 9| CT-p19LC potentiates the effects of erlotinib. Cells were seeded at a density of 4×10^3 A549 cells per well was performed in 96-well plates and left to adhere overnight. In the next day, cells were treated CT-p19LC (10 μM and 20 μM), erlotinib (0,5 μM and 1 μM) or a combination of both. After 72h, cell proliferation was determined by MTT assay. Results are expressed as percentage of cell death relative to the control (untreated cells). Values of A549 cell viability decrease are presented as mean + SD. Yellow represents effect of erlotinib only, blue represents effect of CT-p19LC only, and red represents the percentage of viability decrease which goes beyond the sum of the effects of CT-p19LC and erlotinib combined. Results were compared to erlotinib's solo values by analysis of variance ANOVA using GraphPad Prism (ver 6). (**: $p < 0,01$)..... 42

Figure 10| CT-p19LC treatment impairs proper EGFR response to soluble EGF. Cells were serum starved for 24h, pre-treated with CT-p19LC (20 μM , 2h) and treated with EGF (50 μM) for 30 min. EGF-dependent signaling was evaluated in western blot with EGFR Y¹⁰⁶⁸ antibody. Results are presented as the ratio of band intensity of target protein between CT-p19LC-treated samples and control samples, both normalized to their respective GAPDH band intensity. Quantification of total EGFR and EGFR Y¹⁰⁶⁸ were performed and the difference relating to untreated cells is presented in percentage. 44

Figure_S1| Caveolin-1 levels are different in four adenocarcinoma cell lines. A549, HeLa, MCF-7 and HT-29 human cancer cell lines were grown overnight in 6-well plates with 5×10^5 cells/well. A549 lung cells are the richest in caveolin-1 and in comparison HeLa has less than half of A549 cells' caveolin-1 content and MCF-7 and HT-29 cells' caveoli-1 content are less than 10%. The protein levels were normalized by the respective GAPDH level. b

Figure_S2| Results from MTT proliferation assay performed on lung A549 cancer cell line (above) and breast MCF-7 cancer cell line (bellow) upon treatment with p28, CT-p26, CT-p19 and CT-p19LC in concentrations of 10, 25, 50 and 100 μ M, for 48h.....c

Figure_S3| The effects of erlotinib treatment on A549 human cancer cell line. All these cell lines were seeded overnight in 96-well plates (3 replicates) with a density of 4×10^3 cells per well. Following, these cells were treated with 0,5 1, 5 and 10 μ M of erlotinib during 72 hours. Untreated cells were used as control. d

Index of tables

Table 1 Summarizing list of peptides with description of their selectivity nature, origin, oncolytic properties, clinical progress and reference.	5
Table 2 Summarized list of AntiCP and APD prediction results. Residue substitutions are highlighted and score improvements are in bold.....	27
Table 3 Summarized list of AntiCP prediction results for different improved versions of CT-p26 until final improvement version, CT-p19LC. Residue substitutions are highlighted.....	29
Table_S1 Representation of <i>in silico</i> study on similarity between CT-p26 azurin's region in various <i>Pseudomonas aeruginosa</i> strains where it was concluded that this region is completely conserved within the species.	a

List of abbreviations

α -ACP _{AO}	Selective α -helix anticancer peptide
α -ACP _T	Non-selective α -helix anticancer peptide
β -ACP _{AO}	Selective β -helix anticancer peptide
β -ACP _T	Non-selective β -helix anticancer peptide
ACP	Anticancer peptide
AMP	Antimicrobial peptide
Cav-1	Caveolin-1
cdk2	Cell division-stimulating protein
Cop1	Constitutional morphogenic protein 1
CPP	Cell-penetrating peptide
EGF	Epidermal Growth Factor
EGFR	Epidermal Growth Factor receptor
GAPDH	Glyceraldehyde 3-phosphate dehydrogenase
HDAC	Histone deacetylase
HNP	Human neutrophil peptide
LH/CG	Luteinizing hormone/chorionic gonadotropin
M β CD	Methyl- β -Cyclodextrins
MDR	Multidrug resistance
MTD	Maximum tolerated dose
N-myr-pep	N-myristoylated-peptide
NOAEL	No observed adverse effect level
PS	Phosphatidylserine
TSP-1	Thrombospondin 1
VEGF	Vascular endothelial growth factor

1. Introduction

The contemporary cancer burden has hit an alarming rate since the number of people suffering from a cancer-related disease increases each day. In fact, it is estimated that the number of cancer deaths is going to increase by near 35% in the next two decades. The most probable form of cancer to cause death is lung cancer, which is the more prominently diagnosed in men, followed by liver and stomach cancer. In women, the most prominently diagnosed cancer is breast cancer (WHO 2015) although in European women lung cancer was the most diagnosed in 2016 (Malvezzi et al. 2016).

In some countries of Europe, in the last few years, it is estimated that more people died from cancer than from any other disease, including cardiovascular diseases which are currently considered the major cause of death in developed countries. Also, in the United States it is estimated that in a few years cancer is going to become the major cause of death, surpassing cardiovascular diseases, being already the second most frequent cause of death in children (Nichols et al. 2013; Siegel et al. 2015; Torre et al. 2015). It is suggested that some of the main reasons for this pessimistic statistic are related to unhealthy habits of the general population, to environmental conditions and due to the limitations of conventional anticancer therapies resembling the lack of specificity of some chemotherapeutic drugs, some cases of cancer recurrence and chemotherapeutic drug inefficiency (Gaspar et al. 2013; Torre et al. 2015).

The chemotherapeutic drug armory includes natural products, DNA-alkylating agents, hormone agonist/antagonists, and antimetabolites but all of them presenting insufficient selectivity specially targeting kidney, prostate, bladder and pancreatic cancer cells. Consequently they are nonspecific towards healthy cells presenting the host with deleterious effects such as myelosuppression (decrease production of blood cells) and alopecia (hair loss), two of the most frequently observed (Al-Benna et al. 2011; Riedl et al. 2011). Even some less traditional forms of therapy such as immunotherapy, which is considered a promising approach on cancer therapy, is associated with problems, such as adverse toxicity, reverse autoimmunity and poor tissue penetration (Harris et al. 2011).

The inefficiency of some of these therapeutic choices is also strongly related to cell multidrug resistance mechanisms, most evident in advanced metastatic disease. The increase of membrane transporters, such as efflux transporter, that carry drugs out of the cell is one of the most described MDR mechanisms. Nevertheless, MDR is a multifactorial problem and, as a result, very difficult to overcome. Subsequently, other MDR mechanisms include abnormal expression of drug detoxifying enzymes and defense factors involved in reducing intracellular drug concentration, alteration of drug-target interactions, abnormal tolerance to stress conditions, defects in apoptotic pathways such as aberrant expression of p53 and the increased ability to repair the damage suffered in cell components and macromolecules such as the DNA (Gatti & Zunino 2005; Mader & Hoskin 2006).

Finally, chemotherapeutics inefficiency may also be related to pharmacological factors including inadequate drug concentration at the tumor site which can also contribute to clinical resistance (Allen et al. 2002). There is also emerging evidence that tumors can develop resistance to new lines of treatments such as angiogenesis inhibitors (Mader & Hoskin 2006).

In this context, the demand for new treatment options is indispensable and time is of the essence. The chemotherapy limitations have stimulated the search for new oncolytic agents with different modes of action.

As a result, anticancer peptides have been proved to be a resourceful strategy for the molecularly targeted cancer drug discovery and development process. Peptide-based therapy has numerous advantages over small molecules that involve high specificity, low production cost, high tumor penetration, ease of synthesis and modification (Tyagi et al. 2013). ACPs are reported to have an efficient tissue penetration and uptake by heterogeneous cancer cells, endowed with intrinsic activity or synergizing with existing therapeutics (Gaspar et al. 2013). It is fundamentally expected that peptides result in improved anticancer drugs with higher selectivity for neoplastic cells and reduced damaging effects over healthy tissues. In fact, despite being a novelty, a few natural peptides are now clinically approved as anticancer agents (VanderMolen et al. 2011).

1.1. Anticancer and antimicrobial peptides

Anticancer peptides, or ACPs, are small peptides with lengths reported between 5 to 40 amino acids, a molecular mass less than 10 kDa and a positive net charge at physiological pH. Structurally, ACPs have either α -helix (α -ACPs) or β -sheet (β -ACPs) conformation but some linear and extended structures have already been reported (Hoskin & Ramamoorthy 2008). It is common to find ACPs rich in R, K and P which are hydrophobic amino acids but H and W are also likely to be present. Indeed, anticancer peptides rich in P, called polyproline peptides, can be classified on their membrane-internalization predisposition depending on the specific conformation they adopt given the amount and spatial disposition of P residues (Sanchez-Navarro et al. 2017). High amphipathicity, positive net charge, small size and good balance between hydrophobic and polar regions are the overall physical characteristics for the greater part of both anticancer and antimicrobial peptides that are likely to be important for their function, however there is immense structural diversity yet to be explored (Rodrigues et al. 2009).

To promote the research, education and information exchange of anticancer peptides some bioinformatic tools have been developed (G. Wang et al. 2009). The database APD3 (antimicrobial peptide database) is one of these free access tools, and so, a complete list of anticancer peptides can be accessed in <http://aps.unmc.edu/AP/database/antiC.php>. Also, an anticancer peptide prediction algorithm has been incorporated which has been widely used as an *in silico* approach for drug design.

Accordingly, anticancer peptides are often derived from antimicrobial peptides, or AMPs, which are essentially cationic and hydrophobic in nature (Teixeira et al. 2012; Tyagi et al. 2013). AMPs are expressed in bacteria, fungi, plants and animals such as arthropods, fish, amphibians and mammals. These molecules normally have an important function in host innate immune system against microbial pathogens. AMPs are able to kill a wide range of gram-negative and gram-positive bacteria, fungi,

protozoa and even some viruses. Also, many AMPs are tough immunomodulators, evoking both pro- and anti-inflammatory actions by the host immune system (Zaslhoff 2002; Hoskin & Ramamoorthy 2008).

Antimicrobial peptides obtained either from eukaryotes or bacteria share some common properties. They normally consist of 5–50 amino acid residues, their overall net charge is positive, they are hydrophobic and/or amphiphilic, and they are usually membrane-active (Nes & Holo 2000). However, in respect to both their activity and structure they can be quite different. For instances, bacteriocins are AMPs synthesized by prokaryotes that inhibit or kill phylogenetically related and/or unrelated microorganisms that share the same microbial niche. These peptides have a potential for diversified use in the food and pharmaceutical industries, including, anticancer potential given that some bacteriocin peptides are also anticancer peptides (Paiva et al. 2012; Kaur & Kaur 2015). These microbial-origin molecules often exhibited higher target specificity and stronger potency over those produced by the eukaryotes (Chen et al. 2015). However, some eukaryotic AMPs such as bovine lactoferricin, cecropins and defensins have exhibited unambiguous cytotoxic effect on different types of human cancer cell lines. In fact, cecropins have already shown to kill cancer cells that have resistance mechanisms to conventional chemotherapeutic drugs (Mader & Hoskin 2006). Consequently, these AMPs are very rich in positive charged residues such as R and K, which may be significant to explain the relation between the mode of action against both pathogens and cancer cells (Hoskin & Ramamoorthy 2008).

Nevertheless, not all AMPs present cytotoxicity against cancer cells and not all ACPs were adapted from AMPs. For instance, p28 is a peptide tailored from azurin, a protein of the cupredoxin family expressed in opportunistic pathogen *Pseudomonas aeruginosa* and no antimicrobial actions were widely explored prior to its anticancer potential revelation. This peptide has already passed multiple clinical trials as an ACP (Warso et al. 2013). The reason behind this paradox lies yet to be confirmed but it is expected to have value in the optimization of the process of drug design.

1.2. ACPs as a selective oncolytic therapy

It has been established that tumor cells are up to 50 times more sensitive to lytic peptides than normal cells (Leuschner 2005). Regarding selectivity, ACPs can be classified in two broad categories. The first category contains the group of ACPs (ACP_{AO}) which is active against microbial cells and cancer cells while not being active against healthy mammalian cells. As an example we can look at the ACPs cecropins which are reported to be exclusively cytotoxic against cancer cells and some microorganisms (Hoskin & Ramamoorthy 2008). The second one includes ACPs (ACP_T) that are cytotoxic for bacteria and mammalian cells (Gaspar et al. 2013).

The reason behind ACP_{AO} selectivity is still a controversial topic however some conclusions are evident. Cancer and normal mammalian cells have a number of confirmed differences that are considered responsible for this selectivity phenomenon. The most described differences are membrane-based more

exclusively regarding membrane net negative charge and abnormal fluidity due to change on cholesterol profile which characterizes malignant cells in contrast with healthy mammalian cells (Harris et al. 2011).

Interactions between ACPs and non-malignant mammalian cells are not favored due to the zwitterionic effect present in the membrane of these cells which confers an overall neutral nature. On the contrary, neoplastic cells carry a typical negative net charge due to an abnormal expression of anionic molecules such as phosphatidyl serine (in a proportion of 1:10 of total phospholipids in the membrane), O-glycosylated mucins, sialylated gangliosides and heparin sulfate (Hoskin & Ramamoorthy 2008; Gaspar et al. 2013). In fact, phosphatidyl serine (PS) is a good indicator of cell neoplastic transformation since it will oddly accumulate in the outer leaflet of the membrane unbalancing the charge asymmetric profile.

Regarding fluidity, there is evidence suggesting that cholesterol confers protection to non-malignant cells from the action of α -ACP_{AO} by blocking its access. Indeed, it was found that the presence of lipid rafts rich in cholesterol can be a key factor on differentiating the action and effect of both ACP_{AO} and ACP_T which can also explain their different effect in diverse cancer cell lines depending on their nature of lipid raft constitution. In fact, it was shown that certain tumors, like breast and prostate, present a higher content of cholesterol in the cell membranes (Li et al. 2006). In addition, the abundant presence of microvilli in cancer cells has direct relation to its increased surface area in contrast to healthy mammalian cells. It is suggested that this feature can enhance the toxicity and selectivity of ACP_{AO} due to the possibility of accumulating in higher levels in a bigger cell surface (Harris et al. 2011).

Consequently, these differences may be key to explain why many AMPs present ACP potential considering that microbial membranes also have negative net charge and sterols are absent in bacteria (Hoskin & Ramamoorthy 2008).

A summarizing list of the mainly best described anticancer peptides in the literature is presented in Table 1 along with the information of selectivity, origin, targets, mode of action and study progress respectively for each ACP.

Table 1 | Summarizing list of peptides with description of their selectivity nature, origin, oncolytic properties, clinical progress and reference.

Peptide	Selectivity	Origin	Cancer cells	Anticancer action	Study progress	Reference
A9K	ACP _{AO}	Synthetic	Human cervix and kidney	Both necrosis and apoptosis	Currently, this peptide only appears to have been assayed <i>in vitro</i>	(Xu et al. 2013)
Cecropins A and B	α-ACP _{AO}	<i>Hyalophora cecropia</i> & <i>Musca domestica</i>	Human bladder carcinoma	Depending on cancer cell type: apoptosis or necrosis	These peptides have been assayed both <i>in vitro</i> and <i>in vivo</i> , using murine models (xenografts)	(Hoskin & Ramamoorthy 2008)
D-K ₆ L ₉	ACP _{AO}	Synthetic	Human prostate	Necrosis via membrane depolarization	This peptide have been assayed both <i>in vitro</i> and <i>in vivo</i> , using murine models (xenografts)	(Papo et al. 2006)
Epinecidin-1	α-ACP _{AO}	<i>Epinephelus coloides</i>	Human lung, cervix, liver carcinoma, fibrosarcoma, lymphoma	Depending on cancer cell type: apoptosis or necrosis	Currently, this peptide only appears to have been assayed <i>in vitro</i> (xenografts)	(Chen et al. 2009; Lin et al. 2009)
Gomesin	β-ACP _T	<i>Acanthoscurria gomesiana</i>	Murine subcutaneous melanoma	Membrane permeabilisation via pore formation	This peptide has been assayed <i>in vitro</i> and <i>in vivo</i> using murine models	(Rodrigues et al. 2009)
HNP 1, 2, & 3	β-ACP _T	<i>Homo sapiens</i>	Human lung & Murine colon and breast	Depending on cancer cell type: antiangiogenesis, apoptosis and necrosis	These peptides have been assayed <i>in vitro</i> and HNP-1 <i>in vivo</i> , using murine models (xenografts)	(Droin et al. 2009; Y. S. Wang et al. 2009)
Lactoferricin	ACP _{AO}	<i>Mammalian</i>	Human colon and lung	Antiangiogenesis, apoptosis and lysis by natural killer cells	Currently, the protein is in human clinical trials for non-small cell lung cancer and its peptides have been assayed <i>in vitro</i> and <i>in vivo</i> , using murine models (xenografts)	(Harris et al. 2011)
LL-37	α-ACP _T	<i>Homo sapiens</i>	Human gastric carcinoma	Antimitogenic effect	This peptide has been assayed both <i>in vitro</i> and <i>in vivo</i> , using murine models (xenografts)	(Rodrigues et al. 2009)

Peptide	Selectivity	Nature	Cancer cells	Anticancer action	Study progress	Reference
Magainin	α -ACP _{AO}	<i>Xenopus laevis</i>	Human melanoma & lymphoma	Apoptosis or necrosis	These peptides have been assayed both <i>in vitro</i> and <i>in vivo</i> , using murine models (xenografts)	(Rodrigues et al. 2009)
Melittin	α -ACP _T	<i>Apis mellifera</i>	Human liver carcinoma cells	Apoptosis or necrosis	This peptide has been assayed both <i>in vitro</i> and <i>in vivo</i> , using murine models (xenografts)	(Rodrigues et al. 2009; Xu et al. 2013)
N-myr-pep	ACP _{AO}	<i>Heliothis virescens</i>	Multiple human cell types	DNA synthesis inhibition	Currently, this peptide only appears to have been assayed <i>in vitro</i>	(Ourth 2011)
Polybia-MP1	α -ACP _{AO}	<i>Polybia paulista</i>	Human bladder and prostate	Necrosis	This peptide have been assayed both <i>in vitro</i> and <i>in vivo</i> , using murine models (xenografts)	(Wang et al. 2008)
p28	α -ACP	<i>Pseudomonas aeruginosa</i>	Multiple human solid cancers	p53 restitution	Currently, this peptide passed two human clinical trials	(Warso et al. 2013; Lulla et al. 2016)
Romidepsin	ACP _{AO}	<i>Chromobacterium violaceum</i>	Human lymphoma	HADAC inhibitor	FDA approved anticancer agent for T-cell lymphoma	(VanderMolen et al. 2011)
Tachyplestin I	β -ACP _T	<i>Tachypleus tridentatus</i>	Human prostate, melanoma	Lysis of cancer cell membranes, antiangiogenesis and apoptosis	This peptide has been assayed <i>in vitro</i> and <i>in vivo</i> as RGD-tachyplestin I when injected intraperitoneally into murine models (xenografts)	(Chen et al. 2001)
Temporin1 CEa	α -ACP _T	<i>Rana erythraea</i>	Human breast	Membrane disruption, calcium release, ROS production	Currently, this peptide only appears to have been assayed <i>in vitro</i>	(Wang et al. 2013)

α -ACP_T: non-selective α -helix anticancer peptide; α -ACP_{AO}: selective α -helix anticancer peptide; β -ACP_T: non-selective β -helix anticancer peptide;

1.3. Bioactivity of ACP's against cancer cells

There have been continuous difficulties to empirically confirm ACPs modes of action against malignant cells and the nature of their interactions. Some anticancer peptides were observed to be able to cause membrane disturbance inducing in some cases cell necrosis or apoptosis. In addition, a great part of these peptides have had promising results both *in vitro* and *in vivo*. Regardless its clinical success, other modes of action are described but not yet completely explained and this information would be vital for drug design purposes (Gaspar et al. 2013; Tyagi et al. 2013).

The majority of tests for bioactivity *in vitro* and *in vivo* of anticancer peptides performed up until now were against solid tumors. Solid tumors are masses composed by the malignant cells *per se* and the stroma surrounding them. In carcinomas a third compartment – the basement membrane - often punctuates the space between the malignant cells and the stroma. The carcinoma cells have also the ability to change the nature of this basement membrane in order to easily invade new healthy tissues (Liotta 1984). Carcinomas are currently the most common solid cancers in adults such as cancer of the colon, breast, lung and prostate (Al-Hajj & Clarke 2004). Indeed, it is estimated that breast and prostate cancer counts respectively for 23 and 14% of the total new cancer cases in the last decade (Ferlay et al. 2013).

This tumor masses may contain heterogeneous populations of cells with variable phenotypes which express aberrant differentiation markers that replicate the tissue of origin, as well as cancer cells that have an undeveloped morphology that do not express these markers (Al-Hajj & Clarke 2004).

This phenotypic heterogeneity may be another cause for anticancer therapy failure. If only a portion of the malignant cells present in the solid tumor is capable to proliferate indefinitely and invade the organism, then the goal of anticancer therapy should be to specifically target these actively tumorigenic malignant cells in the whole tumor mass (Tannishtha et al. 2001). Given that metastases are the principal cause of death for patients with solid tumors, is not unusual for patients to relapse years later with distant metastases as a residual number of cancer stem cells persisted after chemotherapy (Liotta 1984; Al-Hajj & Clarke 2004).

Anticancer peptides represent great potential against tumorigenic untargeted cells due to its high tumor cell kill efficiency in very low concentrations doses.

1.3.1. Membranolytic effect based on electrostatic interactions

Membrane disruption is probably the most studied ACP effect in malignant cells. Membranolytic peptides are proved to target different membrane components contributing to their selectivity. Also, their ability to pore formation and targeting may be intimately related to the peptides structure (Teixeira et al. 2012; Gaspar et al. 2013). Consequently, ACPs are also proved to adopt either a bioactive helical conformation at the cell surface or β -sheet structure preceding the engagement with the membrane

(Figure 1). Besides structure, characteristics as positive net charge and presence of hydrophobic residues in high concentrations are also key factors for the membranolytic effect to occur and for the specificity towards cancer cells. In a pioneer study, Sinthuvanich et al, in 2012, proved that folding was vital for the selective lytic effect of the ACP SVS-1 but this was not all (Table 1). This peptide seemed to target malignant cells on the basis of cancer cells negative net charge and showed low micromolar activity against lung carcinoma, epidermal carcinoma and breast adenocarcinoma cell lines, in contrast with non-malignant cell lines on which SVS-1 had little effect.

The same authors have also demonstrated with liposomal leakage assays and electron microscopy the mechanism that involves cancer cell membrane-induced folding of SVS-1 into an amphiphilic β -hairpin capable of interpolating and consequently disrupting the membranes of cancer cells via pore formation, ultimately resulting in cell death. Whereas in healthy cells this effect is minimum due to its neutral net charge which preserves the SVS-1 natural structure (Sinthuvanich et al. 2011). Although the reason behind the electrostatic based targeting was not clear in this study, other studies on representative ACPs have been able to unravel some potential hypothesis. Tests on prostate carcinoma cell line showed that the selectivity of anticancer peptide D-K₆L₉ can be partially attributed to its ability to target surface-exposed PS in cancer cells (Papo et al. 2006).

As explained before, this phospholipid is the major cause for net charge differences between malignant and non-malignant cells becoming an excellent target for selective anticancer drugs. Indeed, *in vivo* studies of the lytic peptide D-K₆L₉ on human prostate and breast xenografts demonstrated that this short membrane-active peptide recognizes and lyses cancer cells of primary tumors and spontaneous experimental metastases thus resulting on tumor growth inhibition (Table 1). Tests in nude mice also proved that D-K₆L₉ lyses tumor cells directly without the involvement of the adaptive immune system (Papo et al. 2006). This study represents a major promise in new forms of anticancer therapy. There is no doubt that with the increasing resistance of cancer against conventional chemotherapy modalities, the D-K₆L₉ peptide has potentially desirable features characterizing a novel anticancer class of drugs. In particular, it has a broad spectrum of activity, acts rapidly, shows synergy with classic chemotherapy, prevents metastases, and does not destroy vital organs (Papo et al. 2006).

Similarly to what has been found in many cases with bacteria treated with this peptide and other cationic variants its drastic membranolytic effect will hopefully complicate the cancer cell's selection of resistant variants (Teixeira et al. 2012).

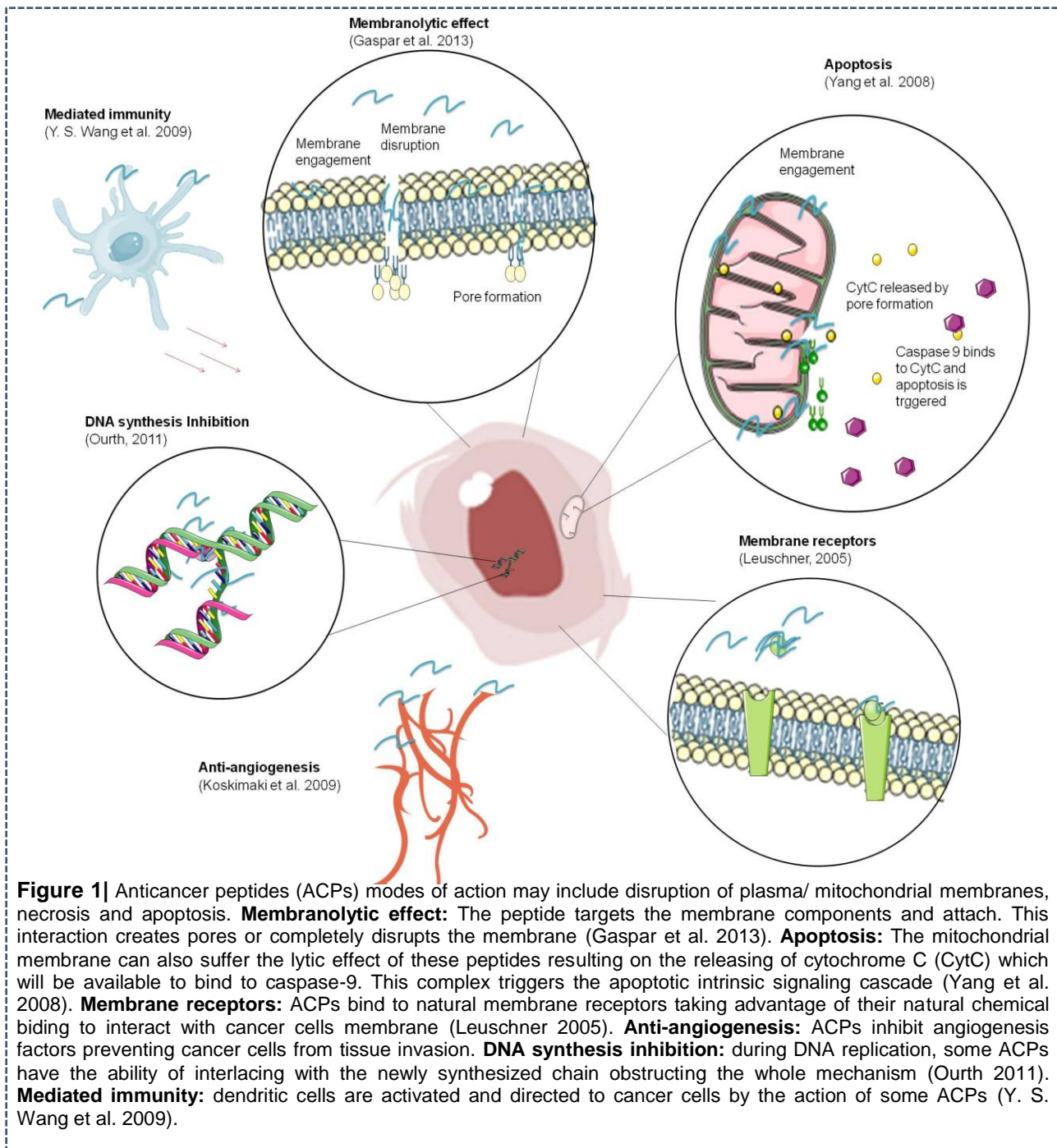
It has been demonstrated that polybia-MPI, a peptide isolated from brazilian wasp venom, selectively inhibited the proliferation of prostate and bladder cancer cells by membrane disruption with low cytotoxicity for normal murine fibroblasts and that the α -helical conformation was an important feature for achieving this anticancer effect (Table 1). Indeed, cytotoxicity was observed in all tested tumor cells and in endothelial cells in a dose-dependent manner. Also, LDH release from normal fibroblasts was relatively much less. These results indicated that polybia-MPI is relatively nontoxic to cells unassociated with tumors and demonstrate cell selectivity.

The dual effect of polybia-MPI that it acts not only on proliferating endothelial cells but also on tumor cells will enhance its antitumor potential (Wang et al. 2008). The study was also important to prove that the role of α -helix structure in the membranolytic effect is vital. The substitution of A by P residues broke the α -helix thoroughly and induced a significant reduction of biological activity of polybia-MPI. Either way, it is clear that polybia-MPI may represent a novel therapeutic strategy, and play a potential role on the treatment of prostate cancer and bladder cancer (Wang et al. 2008). Finally, binding to negatively charged gangliosides expressed on the cell surface can be a potential alternative for directing ACPs activity (Teixeira et al. 2012). Additionally, the lytic effect which already compromises the malignant cells by pore formation in the membranes may also facilitate the entry of other substances such as conventional chemotherapeutic drugs, thus enhancing its efficiency as it will be explored afterward. The pore formation will also represent a challenge to some MDR mechanisms such as efflux pumps (Hilchie et al. 2011).

Apart from the plasmatic membrane, also other biomembranes can suffer the effects of membranolytic peptides. Cancer cells which suffer the action of lytic peptides in their mitochondria may initiate the signaling pathway of apoptosis. Indeed, apoptosis is an essential mechanism that balances cell division and cell death and sustains the appropriate number of cells in the body (Ma et al. 2013). Thus, being a well regulated mechanism, apoptosis is considered a standard strategy in cancer therapy. Until recently, necrosis, unlike apoptosis, was considered an unregulated form of cell death. However, during the last decade a number of experimental data demonstrated that, except under extreme conditions, necrosis may be a well-regulated process, which means it also has potential in cancer therapy (Proskuryakov & Gabai 2010).

Regulatory apoptosis proteins such as Bcl-2 family are controlled by mitochondrial permeability. Anticancer peptides which are able to enter malignant cells and cause membrane pores in the mitochondria trigger the release of its components and liberate Bcl-2. As it can be observed in Figure 1, the recently released cytochrome C forms a complex with caspase-9 initiating a cascade of signals related to apoptosis intrinsic pathway leading to cell death (Huang 2000; Harris et al. 2011; Ausbacher et al. 2012). In situations where the plasmatic and/or mitochondrial membrane is too disrupted, the necrosis mechanism is triggered. More importantly, it is proved that even neoplastic cells with apoptosis mechanism inhibited can still perform necrosis, which is vital for the success of anticancer drugs with both apoptotic and necrotic effect such as Antp and A₉K (Proskuryakov & Gabai 2010; Gaspar et al. 2013).

Indeed, *de novo* designed peptide A₉K have demonstrated to produce cytotoxic effect at low concentrations against cervix cancer cells stimulating cell death by 30% when incubated for only 40 min increasing the cell lethality by only 5% when incubated for further time (Xu et al. 2013). Along with measurements of calcein release, these results prove the strong lytic effect of A₉K in HeLa membranes. In addition, with SEM imaging, HeLa cells were spotted to have apoptotic segments around the cells thus leading to the assumption that this ACP would target internal organelles subsequently to cell penetration.



To further explore the sub-location of A₉K molecules in HeLa cells, a single treated HeLa cell was imaged resulting in proof that A₉K was in fact capable of crossing the cytoplasm and go near the nucleus and mitochondria (Xu et al. 2013). In the same study it was suggested that the mitochondria membrane was a sub-target of this peptide leading to apoptosis when cell membrane disruption damage was not enough to cause necrosis thus the transcriptional levels of bcl-2 gene and c-myc gene were found

consistent with this outcome. In addition, by comparing results with treated normal cells it became clear that the antitumor action of A₉K is achieved through selective membrane binding, resulting in the disruption of cancerous cell membranes, similar mode as observed in its bactericidal attack.

Also, another anticancer peptide with dual effect is proved to trigger apoptosis or necrosis in human gastric cancer cell line depending on the dose administrated (Lee et al. 2015) Calculating those doses may allow the choice of anticancer mode of action and its inherent signaling control. In 2000, Lowe went further and stated that virtually at the right dose all anticancer agents are estimated to induce apoptosis (Lowe & Lin 2000).

1.3.2. Other molecular targets

Anticancer peptides may present alternative pathways to kill tumor cells that do not involve engaging in membrane lyses or apoptosis. Referred targets or mechanisms as represented in Figure 1 are: mediated immunity, hormonal receptors, DNA synthesis inhibition, and anti-angiogenic effects.

It has been proved that anticancer peptide HNP1-3 is associated with necrosis and dendritic cell infiltration in various tumors (Table 1). In 2009, Wang et al. demonstrated that HNP1-3 expressed intratumorally may play a role in the immunity and progression of tumors. The action of this peptide relies on its ability to recruit and activate dendritic cells at tumor sites resulting in inhibition or even eradication of established tumors (Y. S. Wang et al. 2009). Also, this peptide is one of the very few that combine different actions and effects. Specifically, the mediated immunity action is coupled with apoptosis and decreased angiogenesis events (Gaspar et al. 2013). The main reason why HNP (Human neutrophil peptide) is demonstrated to mediate the immune response against tumor sites is due to its natural action. HNPs, also known as α -defensins, are cationic mammal peptides that act against bacteria, fungi, virus and tumors. In fact, upregulation of HNP1-3 in tumor tissue and plasma has been suggested to be a potential marker for prognostic assessment (Droin et al. 2009).

In the same study, Wang et al have demonstrated results derived from an *in vivo* study where intratumoral expression of HNP1 inhibits human lung carcinoma A549 cells xenografts in nude mice. Given that HNPs are chemotactic for human T cells and dendritic cells *in vivo*, HNP1-3 expressed intratumorally may play a role in the immunity and progression of tumors (Y. S. Wang et al. 2009).

Human neutrophil peptide is one of the few human anticancer peptides in study and this fact is accompanied by advantages and disadvantages. It is advantageous when considering that HNP may represent a dual possibility in cancer therapy mode. Because HNP is produced by the patient, its mode of therapy may be included in gene therapy procedures where the tumor surrounding will be modified to overexpress HNP gene. Also, an external administration can be considered as alternative. The disadvantage relies on the fact that being a mammalian molecule thus well known by the organism's system, it could increase the chances of being deactivated by complex biological processes such as

enzymatic hydrolysis or other unknown complications. Also it will be easier for the tumor to produce molecules to enhance HNP degradation as form of resistance (Xu et al. 2013).

Some peptide vaccines have been designed especially to trigger a similar immune response and have hoisted great clinical acceptance, particularly for solid tumors. However the same disadvantages also apply (Purcell et al. 2007).

In Figure 1 is represented a form of ACP action against tumor cells designated membrane receptor. Some hormone receptors such as luteinizing hormone/chorionic gonadotropin (LH/CG) receptors are expressed in prostate, breast, ovarian, testicular, and endometrial cancer cells. Also, they can be up-regulated *in vivo* by treatment with other hormones. Thus it has been demonstrated *in vitro* and *in vivo* in murine models that these cancer cells could be targeted and destroyed by membrane disrupting lytic peptides fused to LH/CG ligands. Also, it was proved that lytic peptide conjugates might be useful for the inhibition of the development of metastases after surgical removal of the primary tumor (Leuschner 2005).

Additionally referring to hormonal receptors, they are not only relevant as targets but as source of ACPs. The ER α 17p peptide is originated from part of the sequence of the estrogen receptor Era. This ACP revealed to interact with the polar part of the plasma cell membrane, to penetrate it and induce cell membrane damage at high concentrations doses (Gaspar et al. 2013).

Undeniable proof about the existence of ACPs mode of actions against cancer cells' DNA has emerged in 2011 thus its representation can be observed in Figure 1. Because of its previous success eradicating some virus such as the cancer promoting double-helix DNA virus Epstein – Barr, the insect N-myristoylated-peptide was isolated by a group of scientists and screened against 56 human tumor cell lines by the National Cancer Institute (Ourth 2011). This peptide was proved to have a cytotoxic effect of more than 60% against 17 different tumor cell lines, both from solid and hematological tumors, in which are included non-small cell lung cancer, leukemia and melanoma along with eight other types of tumor cell lines. Evidence led to the conclusion that the mode of action of this ACP was related to DNA synthesis inhibition hence disturbance on cell growth (Table 1). For the purpose of understanding how this peptide could act against the malignant cells' DNA, its structure was determined. It was concluded that in the C-terminal tail existed a purine-like ring along with two other rings. It is suggested that the DNA base-like chemical signature of this peptide may be the foundation of its DNA synthesis inhibition action (Ourth 2011). This finding was of great importance for ACP drug design.

Finally, tumor progression and metastasis in breast cancer have been shown to be angiogenesis-dependent. Also, the development of other tumors are dependent on neovascular formation (Folkman 1971). Anticancer therapeutic drugs ability to prevent the angiogenesis mechanism in the tumors is of great importance. In fact, endogenous peptides with antiangiogenic activity are considered since 2009 one of the leading tools to treat cancer in addition to other small molecules and antibodies (Koskimaki et al. 2009). The key action of antiangiogenic peptides is to target angiogenesis factors such as the vascular endothelial growth factor (VEGF). These peptides may also be used synergistically along with other forms of therapy. For example, in 2009, Koskimaki et al. proved that peptides derived from type IV collagen,

CXC chemokines and TSP-1 inhibit neovascularization in human breast murine xenographs (Koskimaki et al. 2009). These peptides appeared to target angiogenic factors other than VEGF which means that a possible combination with anti-VEGF antibodies could more efficiently stop localized angiogenesis, thus preventing tumor growth.

1.4. *In silico* drug design of new anticancer peptides

Anticancer peptides have been put on hold in drug development for a long time. The main reasons were the apparent low selectivity of some of the ACPs molecules, the high cost of production in large scale and their low resistance to proteolysis. However, in the last decade the cancer treatment industry have seen new promising peptides being unraveled, thoroughly studied and even approved as anticancer agents. The reasons behind this change were mainly due to the downfall of some conventional chemotherapeutic drugs and tumors' resistance uprising (Gaspar et al. 2013). In addition, it is advantageous that ACPs have excellent malignant tissue penetration, which enables them not only to reach primary but also metastatic tumor sites (Riedl et al. 2011).

Despite the initial lack of rational in designing such peptides given the existence of no link between their structures and their performance, recent studies were able to demonstrate that antibacterial/anticancer peptides share two essential features: they are usually positively charged and tend to fold into amphiphilic structures upon interacting with the target membrane (Chen et al. 2012).

Other features resembling the secondary structure ACPs adopt when in contact with the malignant cell membrane are of importance to drug design since it will most probably play a large role in its selectivity and lytic capacity (Harris et al. 2011).

Drug design is of great importance in the topic of ACPs, even taking into accounts their different nature. It was just a question of time for the creation of bioinformatic algorithms where motifs in the peptides and proteins sequence were associated to specific modes of action or cell targets. Anticancer peptides can either be derived from proteins that usually were also previously studied as anticancer agents or occur naturally as peptides and in both these situations it is possible to benefit from these drug design tools. Soon, the anticancer/antimicrobial peptide field was growing so rapidly in response to demand and *in silico* solutions developed to such predictive capacity levels they were used to improve natural peptides or even create synthetic *de novo* peptide sequences. What began to be a hypothesis improvement solution is now used as a hypothesis originator, coming first to empirical practices (G. Wang et al. 2009).

Now, with the available bioinformatic tools, it is possible to fine-tune every less selective or effective anticancer peptide through simple point modifications *in silico* and screen these modified peptides for anticancer action improvement. In 2003, with the primarily objective of promoting research, education and information exchange in the pharmacological field, APD (antimicrobial peptide database) was formed. This bioinformatic system is dedicated to glossary, nomenclature, classification, information search, prediction,

design, and statistics of both AMPs and ACPs. The information in APD was gathered from the literature (PubMed, PDB, Google, and Swiss-Prot) manually in over a decade, thus this database have expanded tremendously in the passing years (G. Wang et al. 2009). As aforementioned, anticancer peptides mode of action against malignant cells may be related to its structural, chemical characteristics or sequence. Thus, in 2008, Karagiannis and Popel created and tested a bioinformatic tool that could predict peptides derived from several protein families with localized antiangiogenic properties including type IV collagen, CXC chemokines and thrombospondin-1 (TSP-1) domain-containing proteins. The proteome-wide analysis was based on the hypothesis that there is an underlying sequence-based correlation between the activity of the known endogenous protein fragments and the predicted peptides (Karagiannis & Popel 2008; Koskimaki et al. 2009).

Other chemical target which can be explored for anticancer peptide improvement in drug design tools is the amount and organization of P residues. Polyproline anticancer peptides are known to overcome biological barriers more successfully (Sanchez-Navarro et al. 2017). Consequently, an *in silico* tool which strategically organizes or introduce P residues in input sequences may be a good solution to improve anticancer peptide internalization.

In order to use the many *in silico* approaches, the user needs to decide which are the peptide's desired targets and what mode of action it is preferred. For example, if the user has a peptide with demonstrated antiangiogenic potential against malignant cells but low cell invasion rate, then it is possible, using these tools, to create platonic modifications to enhance the peptide lytic capacity. Usually, the algorithm of these drug design tools will give the option for the user to replace more/less hydrophilic amino acids over more/less hydrophobic ones depending on the peptides' original amphipathicity and net charge values (Harris et al. 2011; Tyagi et al. 2013). This is the case of AntiCP, an algorithm designed to distinguish between anticancer peptides and non-anticancer peptides. In 2015, a study validated this algorithm by comparing the cytotoxicity levels of three different peptides derived from VSVG protein. Two of these peptides had scores higher than 0.90 on AntiCP and when tested against MCF-7 and HEK cell lines proved to be effective while the other peptide, with lower AntiCP score proved to have no significant bioactivity against these cancerous cell lines (Ghandehari et al. 2015; Kumar & Li 2017).

To summarize, peptide-based anticancer therapy has gained a tremendous interest in the last decade due to the need of more efficient, easy to produce and antichemoresistance therapy solutions. *In silico* drug design tools have improved tremendously due to this demand and allowed peptide improvement on specific aspects by manipulating several physical and chemical properties such as overall net charge, amphipathicity and peptide length by altering point amino acid residues.

1.5. Peptides tailored from azurin

Azurin, expressed in the opportunistic human pathogen *Pseudomonas aeruginosa*, is a small cooper-binding electron transfer protein derived from the cupredoxin family that has demonstrated multi-

target anticancer activity *in vitro* and *in vivo* (Punj et al. 2004; Bernardes et al. 2016). This protein is composed by 128 amino acids (14 kDa) and comprises eight antiparallel-strands connected by four loops linked by a disulfide bridge (Yamada et al. 2004; Fialho et al. 2016) and azurin's many different domains may be the reason for its different ways of targeting cancer cells and subsequently affect them.

One of the demonstrated cancer cells' targets of this cupredoxin is p53. After targeting and binding to p53, azurin is described to prevent its degradation. Thus, cell cycle is arrested before the mitosis phase which triggers apoptosis. In fact, in a series of studies azurin have demonstrated to trigger cell death both *in vitro* and *in vivo* in breast cell line MCF-7 and in murines with tumors, correspondingly. In addition, azurin was verified to inflict little damage to healthy mammalian cells (Gupta 2002; Punj et al. 2004). This type of cancer targeting performed by azurin has been linked to its domain which comprises p28, which in subsequent work also showed to bind to p53 (Warso et al. 2013), however more details regarding p28 will be given later.

Other works have also suggested that azurin targets the membrane composition of certain types of cancer cells. In 2007, Chaudhari et al. demonstrated that azurin binds to several Eph receptor tyrosine kinases, a family of extracellular receptor proteins known to be unregulated in many tumors, interfering with the cancer cell growing signaling pathway. In fact, the structure of the C-terminal domain of azurin is quite similar to ephrinB2 at the G-H loop region known to be involved in receptor binding. In this work a peptide designed from that region of azurin showed great toxicity levels in prostate cancer cell line (Chaudhari et al. 2007). In 2014, Bernardes et al. revealed that genes related to vesicle transport, lysosomes, endocytosis, membrane organization and endosome transport were up-regulated in a P-cadherin overexpressing breast cancer cell line treated with azurin whereas genes coding for cell surface receptors such as EGFR which usually sustain cell proliferation and aberrant constitutive signaling were down-regulated (Bernardes et al. 2014).

Past work from Taylor et al. have suggested that regarding cell entering, azurin is likely using *caveolae*-mediated endocytic pathways to penetrate through mammalian cells (Taylor et al. 2009) and recent unpublished work from this group have showed that the F residue in azurin's 114 position is vital for this interaction with caveolin-1 to occur (Bernardes et al. 2017 submitted) thus being more cytotoxic than the mutated azurin version with an A residue in that position. The reasoning behind the importance of the F residue in position 114 is the fact that F is a hydrophobic amino acid and hydrophobicity is vital for interactions between some drugs and cancer cell membranes. Indeed, by targeting lipid rafts components, azurin is able to alter membrane packaging levels so cancer cells' membranes become more fluid and thus more susceptible. In fact, azurin has been proved to enhance the anticancer activity of chemotherapeutic drugs such as doxorubicin and paclitaxel which provoke DNA damage (Bernardes et al. 2017 submitted) by turning the cancerous membranes more vulnerable to let anti-DNA chemotherapeutic drugs to perform. Also, other drugs which also target membrane components such as gefitinib and erlotinib are also proved to have its anticancer effect enhanced when in combination with azurin (Bernardes et al. 2016).

1.5.1. p28, a success case in early clinical trials

With the National Service Center code: 745104, p28 is a peptide derived from azurin. This peptide consists on a 28 amino acids portion of azurin, more specifically amino acids 50–77. In terms of structure, p28 assumes conformation of α -helical which coupled with its amphipathic nature facilitates access throughout human cancer cells' membrane. Inside malignant cells, this ACP will be processed into the nucleus where its mode of action will end up increasing intracellular levels of wild-type p53 by binding to its hydrophobic DNA-binding domain, preventing its degradation, as it can be observed in Figure 1 (Warso et al. 2013).

The gene of tumor suppressor protein p53 has been mapped to chromosome 17. In the cell, p53 protein binds to the DNA, which in turn stimulates another gene to produce a protein called p21 that interacts with a cell division-stimulating protein (cdk2). When complex p21-cdk2 is formed, the cell cannot pass through to the next stage of cell division (Kastan & Bartek 2004). The protein p53 is closely regulated by ubiquitylation factors. These factors include constitutional morphogenic protein 1 (Cop1) and HDM2 which are two of the various ubiquitin ligases. These two factors are demonstrated to direct p53 to eventual degradation. A mutation in p53 or its deficiency will lead to the absence of p21 protein and cell division will never stop. Consequently cells will divide uncontrollably, and form tumors (Dornan 2006; Patel & Player 2008).

Nevertheless, *in vitro* studies where wild-type p53 of MCF-7 breast cancer cells was exposed to p28 proved the increase of post-translational levels and activity of p53 which led to the inhibition of the cell cycle at the G2–M transition and induced apoptosis (Yamada et al. 2009). In 2010, *in vivo* studies in preclinical species, with human tumor xenografts also lead to the same conclusion adding that this peptide showed little toxicity in non-malignant cells. All in all, azurine-p28 presented itself as a selective malignant cell-penetrating peptide (CPP) that after entering the nucleus is able to obstruct the binding of Cop1 and HDM2 to p53. These conclusions allowed this peptide to enter clinical trials and be experimented in humans (Jia et al. 2011).

With the FDA's Investigational New Drug (IND) number: 77754, the first azurin-p28 phase I clinical trial ended in 2012 and had the primary objective of determining the No Observed Adverse Effect Level (NOAEL) and maximum tolerated dose (MTD) of intravenous p28 given three times per week for 4 weeks in adult patients with p53-positive advanced solid tumors. Secondary objectives included establishing an appropriate dose for phase II studies, obtaining a pharmacokinetic profile, determining potential immunogenicity and if possible assessing preliminary anticancer activity. All cumulative doses were within or above the levels for preclinical efficacy. All things considered, 15 adult patients with histologically or radiologically proven advanced solid tumors of diverse histogenesis and a possible life expectancy of ± 6 months were accepted in the referred study (Warso et al. 2013).

The second phase I clinical trial ended in 2015 and had the primary objectives of establishing whether the adult recommended phase II dose of p28 was safe for children with recurrent or refractory

CNS tumors and to characterize the serum pharmacokinetics of p28 in children. Secondary objectives were to describe the antitumor activity of p28 in this patient population and characterize the level of p53 expression in available tumors. This study was composed by 18 children aged 3–21 years old with histologically confirmed progressive, recurrent, or refractory high-grade glioma, medulloblastoma, primitive neuroectodermal tumors, atypical teratoid rhabdoid tumor, diffuse intrinsic pontine glioma or choroid plexus carcinoma for whom no curative existing therapy were eligible (Lulla et al. 2016).

Overall, the clinical trial in adults did not report any dose-limiting toxicities or significant incidents in the 15 participants enrolled. Best responses included 1 complete response, 3 partial responses and 7 patients with stable disease. Three participants with melanoma or colon cancer were alive at 25, 32, and 36 months after therapy completion (Warso et al. 2013). The clinical trial in children with CNS tumors revealed that the single most common adverse event attributed to the drug was transient grade 1 infusion-related reaction. Pharmacokinetics analysis revealed a profile similar to adults; however higher p53 expression in tumor cell nuclei was observed in 6 of 12 available tissue samples. There were no objective responses; 2 participants remained stable on the study for 4 cycles (Lulla et al. 2016).

As a final point, as a single anticancer agent, p28 is not likely to be effective against pediatric CNS tumors yet a more optimistic anticancer potential was observed in the first clinical trial against solid malignancies. Still, further combination strategies are being explored preclinically (Lulla et al. 2016). All things considered, p28 have showed to be a safe and selective anticancer agent. It is considered nowadays the lead agent in a series of cell-penetrating peptides that enhance the stability of p53. There are up until now four active patents on p28 as an anticancer peptide (Fialho et al. 2012)

1.5.2. CT-p26 is active against epithelial tumor cell lines

As mentioned before, other domains in azurin have also demonstrated putative anticancer potential (Chakrabarty et al. 2014). If in one hand p28 seems to be linked to azurins capacity of p53 targeting in another hand a recent study of Bernardes et al. 2017 (submitted) has shown significant evidence that a specific region near azurin's C-terminal extremity is essential to cancer cells' plasmatic membrane's targeting and penetration. In assays where azurin WT was compared to azurin F114A, significant data showed that the aromatic properties of F residue in azurin's 114 position are key to the membrane-targeting anticancer potential of this cupredoxin since its substitution for an A residue showed a clear decrease in the cytotoxic capacity of this mutant against cancer cells when comparing with the wild-type. In all the used concentrations, azurin F114A has a reduced entry capacity when compared to the azurin WT, thereby suggesting that this hydrophobic residue might play a role in the first recognition steps between azurin and *caveolae*, and that this interaction is probably critical to the entry of this bacterial protein in cancer cells. In addition, upon treatment with F114A azurin the effect in the lipid rafts seemed less accentuated which suggested that F114A azurin has poor penetration capacity in cancer cells. Also, it suggested that this hydrophobic domain of azurin is vital for its entry and the disruption of *caveolae* in the membranes of cancer cells (Bernardes et al. 2017 submitted).

With that in mind, a peptide designed from the C-terminal domain of azurin comprising F residue in the 114 position was synthesized and named CT-p26 and subsequently tested showing promising bioactivity against tumor cell lines.

1.5.3. Lipid rafts' components and potential therapeutic targets

Located in the plasmatic membrane, lipid rafts operate as platforms for cell signaling. These microdomains are divided into two types: planar lipid rafts and non-planar lipid rafts and are less fluid than the surrounding bulk of the membrane's paraphernalia. They are enriched in cholesterol, sphingolipids and certain types of proteins. Melanomas, prostate, and breast cancers are registered to have increased levels of lipid rafts which suggests that these structures may play a functional role during tumorigenesis (Murai 2015).

Caveolae represent a morphologically identifiable subset of lipid rafts. In fact, caveolar lipid rafts were the first lipid rafts to be discovered because they could be observed by electron microscopy. While the overall biochemical composition of lipid rafts and *caveolae* is thought to overlap, these microdomains are not completely equivalent (Cohen et al. 2004).

Caveolins are the main integral proteins of *caveolae*. They are essential for the invagination of the plasma membrane through a largely unknown process, giving them their characteristic flasklike appearance. Adding, they tightly bind cholesterol and sphingolipids and they cannot be dissociated by high levels of salts or non-ionic surfactant detergents (Rothberg et al. 1992). Indeed, caveolins play an important role in cholesterol trafficking, a key component in lipid rafts (Martinez-outschoorn et al. 2015).

There are several gene families of caveolins but it is CAV1 expression that is regulated by cholesterol. In fact, several studies have revealed the importance of Cav-1 during the process of tumor progression and its expression was detected in different types of tumors. Indeed, Cav-1 regulates multiple cancer-associated processes including cellular transformation, tumor growth, cell death and survival, multidrug resistance, angiogenesis, cell migration, invasion, apoptosis and metastasis. However, it is evident that Cav-1 also acts as a tumor suppressor (Williams et al. 2004).

The expression of caveolins varies widely but a total absence of caveolins is rare. In fact, Cav-1 is expressed at different levels in multiple tissues, with the highest levels found in adipocytes, endothelial cells, fibroblasts, smooth muscle cells, and a variety of epithelial cells (Martinez-outschoorn et al. 2015).

Cav-1 also interacts with other lipid rafts proteins such as G proteins, G protein-coupled receptors, RAS family members, RHO family GTPases, adenylate cyclase isoforms and a series of kinases, such as SRC family members and EGFR. The Epidermal Growth Factor Receptor (EGFR), when activated, stimulates signaling pathways involved in cell growth, survival and migration (Quest et al. 2008).

Several agents of the chemotherapeutic paraphernalia have recently been found to inhibit tumor cell proliferation or invasiveness by targeting membrane rafts such as gefitinib and erlotinib which are drugs who target EGFR (Yang et al. 2017).

2. Objectives and thesis outline

The primary objective of this thesis was to improve the efficacy and specificity against tumor cells of CT-p26 using *in silico* optimization tools preferentially reducing its sequence length to decrease synthesis burden and associated costs and also optimize some intrinsic characteristics that would simplify its experimental handling, such as solubility, in order to hopefully improve results.

The subsequent objectives were to test the resulting peptide of the predictive optimization tools against cancer cell lines to attest to its cytotoxicity and against non-malignant cell lines to study its selectivity potential. The cancer cell lines used as study object were from breast, lung, colorectal and cervix adenocarcinoma. The decision to study the new improved peptide against solid tumor cell lines were based on the previous promising experiments of CT-p26, a peptide tailored from azurin, against lung and breast adenocarcinoma. This decision is also based on the assumptive membranolytic potential of this new peptide given the design targets chosen in the *in silico* tools: higher amphipathicity and positive net charge. These characteristics have been extensively associated with cell penetrating peptides and the overall peptide capacity for cell membrane pore formation and necrosis (Boohaker et al. 2015).

As introduced, membrane fluidity plays an important role on cancer cells drug resistance and on the targeting of the same cells by anticancer drugs with high specificity. Indeed, several physiological processes including cholesterol metabolism and membrane fluidity signaling are proved to be important in breast and colon cancer development and therapy resistance (Kloudova et al. 2017). Accordingly, data regarding azurin's effect on lung cancer cells membrane fluidity was reported by Bernardes et al. 2017 (submitted). As a result, in the domain of this thesis, to further study the effect of CT-p19LC on membrane order, a methodology using fluorescent probes along with use of confocal microscopy was performed on the cancer cell lines when treated and compared to untreated cells.

Finally, given that it has been widely demonstrated that azurin and p28 enhance the effect of several chemotherapeutic and small chemical inhibitor drugs some of which target EGFR such as erlotinib and gefitinib, it is relevant to confirm a possible synergistic effect between CT-p19LC and erlotinib. Also, western blot analysis were performed on A549 lung cancer cells to study the effect of CT-p19LC, erlotinib or both on EGFR levels which may give some clues about CT-p19LC target and mode of action.

3. Materials and methods

3.1. *In silico* analysis

Azurin protein sequences from all considered species in the query of the study were obtained from NCBI - National Center for Biotechnology Information (<https://www.ncbi.nlm.nih.gov/>) and aligned using standard protein blast tool (blastp) from the same source (<https://blast.ncbi.nlm.nih.gov/Blast.cgi>).

Peptide optimization was performed by two different bioinformatic tools. The first predictive tool was the peptide algorithm AntiCP from the Institute of Microbial Technology in India (<http://crdd.osdd.net/raghava/anticp/>). The second predictive tool was the Antimicrobial peptide database and its incorporated algorithm (<http://aps.unmc.edu/AP/main.php>). Innovagen™ peptide property calculator algorithm was used to predict the solubility potential of the query peptides (<http://pepcalc.com>).

For both peptide optimization algorithms and Innovagen's calculator, the input was the FASTA sequence of CT-p26 and the comparable 26 residue-portion from all other different azurins and afterward the FASTA sequence of the shortened versions.

3.2. Peptides

Within the domain of this Microbiology thesis, two peptides (CT-p19 and CT-p19LC) were designed and their synthesis was ordered from Pepmic Co., Ltd. Lyophilized samples of CT-p19 and CT-p19LC was dissolved in 10 mM phosphate buffer (pH 7.4).

In addition, synthesis of CT-p26 and p28 were ordered from Pepmic Co., Ltd, and were dissolved in PBS – Phosphate buffer saline (pH 7.4).

3.3. Cell culture

Human epithelial cancer cell lines A549 (lung), HeLa (cervix), HT-29 (colorectal) and MCF-7 (breast) were obtained from ECACC (European Collection Of Authenticated Cell Cultures). They were maintained in DMEM-Dulbecco's Modified Eagle Medium (Gibco® by Life Technologies), supplemented with 10% of heat-inactivated Fetal Bovine Serum (Gibco® by Life Technologies), 100 IU/ml penicillin and 100 mg/ml streptomycin (PenStrep, Invitrogen). These cell lines were sub-cultured between 2 to 3 times per week, by chemical detaching with 0.05% trypsin.

Human bronchial cell culture 16HBE14 was grown in MEM without Earls salts supplemented with 10% of Fetal Bovine Serum, 1% of L-glutamine and 10000 U/ml penicillin and 10000 mcg/ml streptomycin (PenStrep, Invitrogen). This cell line was cultured in fibronectin coated T-flasks. Sub-culturing was performed by chemical detaching with 0.05% trypsin followed by spin at 1200 rpm.

Human mammary gland cell line MCF-10A was cultured in MBEM (Lonza Co.). The sub-culture is performed by detaching with 0.05% trypsin for 15 minutes following trypsin neutralization by addition of 3 ml solution of 0.1% soybean trypsin inhibitor (ATCC® 30-2014™). Centrifugation of cell suspension was performed at 1200 rpm for 5 minutes. The culture conditions for all cell lines were 37°C in a humidified chamber containing 5% of CO₂ (Binder CO₂ incubator C150).

3.4. MTT cell proliferation assay

Solo assays: MTT [3-(4,5 dimethylthiazol-2-yl-2,5 tetrazolium bromide)] assays were used to determine the viability of human A549 (lung), HeLa (cervix), HT-29 (colorectal) and MCF-7 (breast) adenocarcinoma cells as also 16HBE14 non-cancer bronchial cells and MCF-10A non-cancer breast cells exposure to the effects of azurin's peptides CT-p26, p28 or CT-p19 and CT-p19LC. Cancer cell lines were seeded in 96-well plates (Orange Scientific), in 3x replicates per well, at a density of 10⁴ cells per well and were left to adhere and grow overnight in a CO₂ incubator (5%) at 37°C. The 16HBE14 and MCF-10A cells were seeded in 96-well plates (Orange Scientific), in 3x replicates per well, at a density of 7,5x10⁴ and 4,5x10⁴ cells per well, respectively, and were left to adhere and grow in the same conditions. In the next day, medium was collected and cells were treated with 0 µM; 10 µM; 25 µM; 50 µM and 100 µM of p28 or CT-p26; or with 0 µM; 2,5 µM; 5 µM; 7 µM ;10 µM; 25 µM; 30 µM; 50 µM and 100 µM of CT-p19LC and were left for 48 h in the same growth conditions.

Combination assays: MTT [3-(4,5 dimethylthiazol-2-yl-2,5 tetrazolium bromide)] assays were used to determine the viability of A549 lung cancer cells upon CT-p19LC and erlotinib exposure. Lung A549 cancer cells were seeded in 96-well plates (Orange Scientific), in 3x replicates per well, at a density of 10⁴ cells. After 24 h, medium was changed and fresh CT-p19LC, erlotinib (Santa Cruz), a combination of both or an identical volume of media with buffer were added and were left for 72 h in the same growth conditions.

After this time, 20 µL of MTT reagent (5 mg/ml) was supplemented to each well and incubated for 3.5 hours. The reaction was stopped by the addition of 40 mM HCl in isopropanol (150 µL). MTT formazan formed was spectrophotometrically read at 590 nm in a 96-well plate reader (SpectroStarNano, BMG LABTECH). Untreated cells were used as control, in order to determine the relative cell viability of treated cells.

3.5. Two-photon excitation microscopy – GP determination

The human A549 (lung), HeLa (cervix), HT-29 (colorectal) and MCF-7 (breast) adenocarcinoma cells were cultured on µ-Slide 8 well glass bottom chambers (ibidi®) with 5x10⁴ cells and treated with CT-p19LC (20 µM). After 2 h, medium was collected and cells were washed twice with PBS. After that,

medium was renewed containing 5 μM of Laurdan's and the cells were incubated in a CO_2 incubator at 37°C for 15 min (Binder CO_2 incubator C150). Untreated cells were the control condition.

Samples were examined on a Leica TCS SP5 (Leica Microsystems CMS GmbH, Mannheim, Germany) inverted microscope (model no.DMI6000) with a 63 \times water (1.2-numerical-aperture) apochromatic objective. Two photon excitation data were obtained by using Leica TCS SP5 inverted microscope with a titanium-sapphire laser as the excitation light source. The excitation wavelength was set to 780 nm and the fluorescence emission was collected at 400–460 nm and 470–550 nm to calculate the GP images. Laurdan's GP images were obtained through homemade software based on a MATLAB environment.

3.6. Antibodies

The following antibodies were used: GAPDH (Glyceraldehyde 3-phosphate dehydrogenase 1:1000, Santa Cruz Biotechnology), Epidermal growth factor receptor (1:500, Cell Signaling) and pEGFR -Y1068 (1:500, Cell signaling).

3.7. Protein extraction and Western blot

The A549 cancer cells cultured in 6-well plates were serum-starved for 24 h prior to treatment with 20 μM of CT-p19LC for 2 h. EGFR signalling was stimulated by the addition of EGF (50 ng/mL), for 30 minutes. Non-stimulated cells represent control. All incubation time was at 37°C in a 5% CO_2 atmosphere. For protein extraction the wells were washed twice with PBS 1x. Cell lyses was achieved using 100 μL of Catenin Lysis Buffer (CLB; 1% Triton X-100, 1% Nonidet-P40 in PBS) supplemented with 1:7 proteases inhibitor (Roche Diagnostics GmbH) and 1:100 phosphatases inhibitor (Cocktail 3, Sigma Aldrich) for 10 minutes at 4°C . The cells extracts were scratched, collected and vortexed three times (10 seconds each), centrifuged (14000 rpm, 4°C , 10 min; B. Braun Sigma-Aldrich 2K15) and the pellet was discarded, collecting the supernatant containing proteins.

The samples were quantified by a Quantification Protein Kit (Bradford, BioRad). The determination of the total protein concentration, per sample, was achieved through the use of a calibration curve, on which were used the absorbance values of standard samples of bovine serum albumin (BSA), whose concentrations are known (provided by the kit). The Bradford method is based on the observation that Comassie Brilliant Blue G-250 exists in two different color forms, red and blue. The red form is converted to the blue form upon binding of the dye to protein. The protein-dye complex has a high extinction coefficient thus leading to great sensitivity in measurement of the protein (Bradford 1976). Final quantification of 40 μg (EGFR phosphorylated protein form) and 15 μg (EGFR) of the total protein lysate was dissolved in sample buffer [Laemmli with 5% (v/v) 2- β -mercaptoethanol and 5% (v/v) bromophenol blue and boiled for 5 min at 95°C].

Following, the proteins were separated by electrophoresis in SDS-PAGE gels with 8% acrilamide and 10% SDS. The human epidermal growth factor receptor (EGFR) and its phosphorylated form weight approximately 132 KDa, being better resolved in a less thick acrilamide. The resulting SDS-PAGE gel was electrically transferred to a nitrocellulose membrane (RTA Transfer Kit, BioRad), using a Trans-Blot® Turbo Transfer System (BioRad) and applying the manufacturer's instructions. After blocking the non-specific binding sites for 1 h with 5% (w/v) not-fat dry milk in PBS-tween-20 (for the non-phosphorylated protein form) and with 5% (w/v) BSA (for the phosphorylated protein form), the membranes were incubated in an agitator overnight at 4°C with different primary antibodies (anti-EGFR diluted 1:500 in 5% non-fat milk, anti-pEGFR-Y¹⁰⁶⁸ diluted 1:500 in 5% BSA and anti-GAPDH diluted 1:1000 in 5% non-fat milk buffer).

In the next day, the membranes were washed three times with PBS tween-20 (0.5% v/v) for 5 min and probed with the appropriated secondary antibody, conjugated with horseradish peroxidase [anti-rabbit (sc-2354, Santa Cruz Biotechnology), EGFR, and its phosphorylated form, diluted 1:2000 in 0.5% PSB tween-20, and anti-mouse (sc-2005, Santa Cruz Biotechnology) for GAPDH at room temperature for 1 h, in an agitator. After washed, the membranes were revealed by adding ECL substrates (Pierce) and capture the chemiluminescence by Fusion Solo (Vilber Lourmat) equipment.

3.8. Statistical analysis

For *in vitro* experiments, at least one independent replicate were performed (n=1 to 5 sample/experiment). Experiments performed once were considered preliminary results. For, GP comparison was calculated by student's t-test (two tailed distribution, two sample equal variance). For MTT proliferation assays, results were compared by analysis of variance ANOVA (using GraphPad Prism ver 6). Values of $p < 0.05$ were considered statistically significant (*: $p < 0.05$).

4. Results and discussion

4.1. Cytotoxic effect of azurin and derived peptides on cancer cells

The primary evidences that CT-p26, derived from the C-terminal extremity of azurin, is of interest to further investigation of its anticancer potential are shown in Figure 2. MTT proliferation assays demonstrated that CT-p26 appears to be at least 10% more active against breast cancer cells (MCF-7) than azurin itself, in the same concentrations (100 μ M). Also, p28, another azurin tailored peptide, appears to be 10 to 15% less cytotoxic than CT-p26 against both lung and breast cancer cells (A549 and MCF-7, respectively), also in the same concentration of 100 μ M. These results are the foundation of this thesis premise and primary objective of re-designing the C-terminal extremity of azurin, which comprises CT-p26, with the aim of decreasing its length, improving its solubility and anticancer effect.

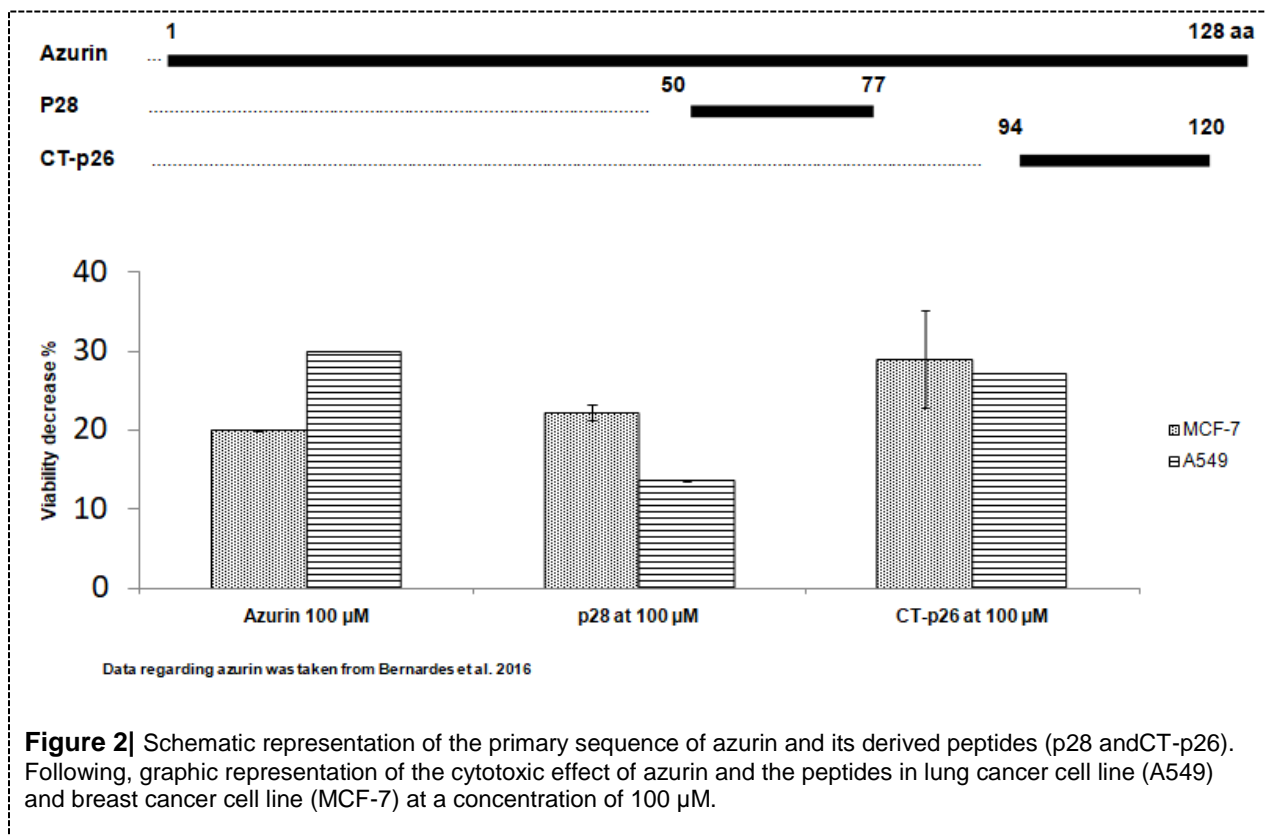


Figure 2| Schematic representation of the primary sequence of azurin and its derived peptides (p28 and CT-p26). Following, graphic representation of the cytotoxic effect of azurin and the peptides in lung cancer cell line (A549) and breast cancer cell line (MCF-7) at a concentration of 100 μ M.

Nevertheless, it is intuitive to assume that p28 could also be eligible for the same kind of redesign however our focus remains on the C-terminal domain of azurin which we have reasons to believe it is vital for azurin's capacity of targeting cancer membranes as a subsequent result of the work performed by this group (Bernardes et al. 2017 submitted). Also, the anticancer peptides' optimization algorithms are more

prepared to design peptides with membranolytic action instead of peptides which target and bind to tumor suppressor proteins, which is believed to be the category p28 falls into.

4.2. *In silico* optimization of CT-p26

4.2.1. Computational study of CT-p26

The sequence of peptide CT-p26 is derived from azurin of *Pseudomonas aeruginosa* PAO1. A preliminary computational study of azurin's CT-p26 fragment diversity was required prior to its attempt for redesign and optimization. We aimed for some conclusions in this preliminary study about the region of azurin comprising CT-p26 level of conservation among the species and other genus from different environmental circumstances. Consequently, in the presence of conserved residues we aimed to understand its relevance regarding the proteins action on the topic of its hydrophobicity or other aspects with potential concern to anticancer capacity. Azurin's region comprising CT-p26 (from 94-120 amino acids) is a conserved sequence among general *Pseudomonas aeruginosa* strains and not particular of PAO1 strain. This was asserted in this thesis project, using NCBI to obtain the protein sequences and blastp algorithm where *P. aeruginosa* azurin amino acid sequences from 17 different strains were aligned against azurin sequence from *P. aeruginosa* PAO1. This result (Table_S1) enabled us to pursue this *in silico* study with the original sequence from our model and consequently the strain specification will no longer be referred for simplification reasons. A second blast alignment was performed with a broader sample composed by a very diverse group of bacteria that expressed azurin. This group varied from human pathogens to bacteria with environmental relevance. In this analysis, azurin sequence from different bacteria were aligned and compared with the azurin sequence derived from *Pseudomonas aeruginosa*. The underline objective of this investigation was to seek for differences in these sequences that may represent anticancer potential. The blast analysis on this representative sample showed very significant information (Table 2). As expected, azurin's residues from 94 to 120 in *Pseudomonas aeruginosa* (CT-p26) share more similarities within the *Pseudomonas* genus. Yet, the sequences of other genus revealed also very similar regions when comparing all sequences, which repeated in almost all sample in the same positions. Indeed, one example is 108^{*} tyrosine residue that seems to be conserved in almost all sample yet in an isolated fashion. This residue is supposed to play a significant role in the structural folding of azurin given its Greek key similar shape. It is demonstrated that the group of proteins with this structural shape have an important isolated tyrosine that is referred as tyrosine corner (Hamill et al. 2000). However, it is unlikely, given the peptide's small length, that this residue would play an important role on CT-p26 anticancer action, so no particular determinant differences were registered regarding the different azurins that could indicate more putative anticancer potential comparing to the sequence of CT-p26.

To explore the anticancer potential of the query sequences two different anticancer peptide prediction algorithm tools were used. The available bioinformatic tools allow the fine-tuning of existing peptides or even *de novo* construction of new ones. AntiCP is an online prediction server linked to a database with more than 200 registered peptides with documented anticancer properties (Tyagi et al. 2013). Also, APD, a general antimicrobial peptides database has a similar predictive tool (G. Wang et al. 2009). With the sequences in study as input, the anticancer potential of these peptides was calculated by both algorithms along with suggested optimizations which correspond to single residue modifications (Table 2).

Both AntiCP and APD algorithms predicted anticancer potential in all peptides tested. AntiCP, as an output, give quantifiable final scores where 1.00 is the maximum score which means maximum anticancer potential and -1.00 is the lowest which means it does not have anticancer potential. As a threshold for anticancer potential we used 0.50, below which the algorithm would not consider the sequence an anticancer peptide. In the literature the values diverge although a validation study performed in 2015 by Ghandehari et al. proved that a peptide with lower AntiCP score than 0.50 was non-effective against MCF-7 breast adenocarcinoma cells, so the reference value of 0.50 was decided based on the algorithm's suggestion, based on prior validation studies and also based on the fact that the original CT-p26 had a score of 0.76 and we already had preliminary proof of its anticancer effect *in vitro*. In Table 2 we can see that all sequences without improvement have values above 0.50 which mean they all have the hydrophobicity and/or net charge values that entail anticancer potential to peptides.

Regarding APD, this algorithm is not built to give a quantifiable score, but instead it will directly inform the user if the tested sequence has anticancer/antimicrobial potential. All sequences in their natural form were considered peptides with anticancer/antimicrobial potential by this algorithm, which means that APD and AntiCP algorithms may have into account similar variables regarding anticancer peptides' classification and prediction. Indeed, these algorithms also give as outputs other information regarding the chemical profile of the tested peptides. Cancer and normal mammalian cells have a number of confirmed differences that are considered responsible for anticancer peptide efficacy. The most described differences are membrane-based more utterly regarding membrane net negative charge and abnormal fluidity due to change on cholesterol profile which characterizes malignant cells in contrast with healthy mammalian cells (Harris et al. 2011). As a result, previous studies of Harris et al. and Teixeira et al. have proved that characteristics such as positive net charge, amphipathicity and a balanced ratio between hydrophobic and hydrophilic residues are the key factors conferring anticancer properties for the larger group of both antimicrobial and anticancer peptides (Harris et al. 2011; Teixeira et al. 2012). Consequently, these algorithms will use these quantifiable characteristics as variables when analyzing the peptide sequence given the nature of its residues in order to classify, predict and improve these peptides regarding anticancer potential.

Table 2 | Summarized list of AntiCP and APD prediction results. Residue substitutions are highlighted and score improvements are in bold. Values of charge represented at physiological pH.

Organism	Input sequence	AntiCP					APD		
		Score	Hydrophobicity	Hydropathicity	Amphipathicity	Hydrophilicity	Charge	Hydrophobicity Ratio (%)	Charge
<i>P. aeruginosa</i> (CT-p26)	VTFDVS K LKEGEQYMFCTFP G H S A L	0.76	-0.03	0.07	0.48	-0.28	-0.5	42	0
	VTFK V S L K K GEQYMFCTFP G H S A L	0.85	-0.06	-0.03	0.72	-0.28	3.5	42	4
<i>Pseudomonas fluorescens</i> S613	VTFDVS K LDAAEKYGFFCSF P G H I S M	0.77	0.01	0.29	0.39	-0.28	-0.5	46	0
	VTF V S K LDAAEKYGFFCSF P G H I S M	0.82	0.06	0.59	0.39	-0.45	0.5	50	1
<i>Pseudomonas chlororaphis</i> PCL1606	VTFDVS K LTAGESYEFFCSF P G H N S M	0.76	-0.02	0.01	0.29	-0.30	-1.5	38	-1
	VTFDVS K L L AGESYEFFCSF P G H N S M	0.81	0	0.18	0.29	-0.35	-1.5	42	-1
<i>Pseudomonas flexibilis</i> ATCC 29606	VTFDVAQLQADGQYMFCTFP G H A A V	0.77	0.07	0.52	0.20	-0.73	-1.5	53	-1
	VTFD V LQLQADGQYMFCTFP G H A A V	0.83	0.08	0.59	0.20	-0.73	-1.5	53	-1
<i>Pseudomonas fuscovaginae</i> IRR1 6609	VTFDVS K LNP A EKYGFFCSF P G H I S M	0.75	0	0.16	0.39	-0.37	0.5	42	1
	VTF C V S KLNP A EKYGFFCSF P G H I S M	0.80	0.03	0.39	0.39	-0.52	1.5	46	2
<i>Pseudomonas putida</i> W619	VKFDTS K L E AGGDYSFFCTFP G H I S M	0.75	-0.02	0.02	0.39	-0.22	-0.5	38	0
	VKFDTS K K EAGGDYSFFCTFP G H I S M	0.80	-0.09	-0.28	0.53	-0.03	0.5	34	1
<i>Pseudomonas corrugata</i> RM1-1-4	VTFDVS K LDAAEKYGFFCSF P G H I S M	0.77	0.01	0.29	0.39	-0.28	-0.5	46	0
	VTF V S K LDAAEKYGFFCSF P G H I S M	0.82	0.06	0.59	0.39	-0.45	0.5	50	1
<i>Pseudomonas mosselii</i> Gil3	VKFDAT K L E AGGDYSFFCTFP G H I A M	0.74	0.02	0.22	0.39	-0.28	-0.5	46	0
	VKFDAT K L V AGGDYSFFCTFP G H I A M	0.78	0.06	0.52	0.34	-0.45	0.5	50	1
<i>Pseudomonas alcaligenes</i> OT 69	TTIDVS K L A AGESYEFFCSF P G H V S M	0.70	0.01	0.28	0.29	-0.30	-1.5	42	-1
	TTIDVS K L V AGESYEFFCSF P G H V S M	0.78	0.03	0.37	0.29	-0.34	-1.5	42	-1
<i>Neisseria meningitidis</i> M07165	LTLDP A KLADGDYKFACTFP G H G A L	0.66	-0.02	0.08	0.35	-0.15	-0.5	44	0
	LTLDP L KLADGDYKFACTFP G H G A L	0.73	0	0.16	0.35	-0.20	-0.5	44	0
<i>Neisseria gonorrhoeae</i> 32867	LTLDP A KLADGDYKFACTFP G H G A L	0.66	-0.02	0.08	0.35	-0.15	-0.5	44	0
	LTLDP L KLADGDYKFACTFP G H G A L	0.73	0	0.16	0.35	-0.20	-0.5	44	0
<i>Kangiella sediminilitoris</i> KCTC 23892	ISFTIDEAGTYEYICTFP G H Y F M	0.87	0.07	0.23	0.17	-0.65	-2.5	39	-2
	ISFTIDEA C TYEYICTFP G H Y F M	0.94	0.07	0.35	0.17	-0.70	-2.5	43	-2
<i>Bordetella bronchiseptica</i>	VTFDVA K L A AGDDYTF F C S F P G H G A L	0.69	0.07	0.50	0.20	-0.42	-1.5	50	-1
	VTFDVA K L L AGDDYTF F C S F P G H G A L	0.77	0.08	0.58	0.20	-0.47	-1.5	50	-1
<i>Rhodanobacter denitrificans</i> FW104-R3	ATINV T KLKAGEQYAYFCTFP G H A A L	0.74	0	0.18	0.43	-0.47	1.5	46	2
	ATINV T E LKAGEQYAYFCTFP G H A A L	0.80	0.02	0.20	0.34	-0.47	-0.5	46	0
<i>Achromobacter xylosoxidans</i> KCJK1726	VTFDVS K L A AGQDYAYFCSF P G H F A L	0.73	0.06	0.46	0.24	-0.59	-0.5	50	0
	VTFDVS K L L AGQDYAYFCSF P G H F A L	0.81	0.07	0.54	0.24	-0.64	-0.5	50	0
<i>Vibrio parahaemolyticus</i> KvP10	ITFSTE K MTAGGDYSFFCSF P G H W A I	0.74	0.05	0.18	0.25	-0.55	-0.5	42	0
	ITF C TEKMTAGGDYSFFCSF P G H W A I	0.82	0.06	0.30	0.25	-0.60	-0.5	46	0
<i>Vibrio natriegens</i> CCUG 16374	ITFSTE K MTAGGDYSFFCSF P G H W A V	0.74	0.04	0.17	0.25	-0.54	-0.5	42	0
	ITF C TEKMTAGGDYSFFCSF P G H W A V	0.82	0.06	0.29	0.25	-0.59	-0.5	46	0
<i>Aeromonas hydrophila</i> 2010	VTFKTD G L A GKDLTF F C S F P G H F A M	0.69	0.04	0.40	0.35	-0.41	0.5	48	1
	VTFKTD G L A K KDLTF F C S F P G H F A M	0.81	-0.01	0.26	0.50	-0.29	1.5	48	2
<i>Xanthomonas euvesicatoria</i> LMG 933	VSFPT S KL S KGADYTF F C S F P G H W A M	0.82	0.01	0.07	0.34	-0.55	1.5	42	2
	VSF V TSKLSKGADYTF F C S F P G H W A M	0.85	0.03	0.30	0.34	-0.57	1.5	46	2

In Table 2 is possible to analyze the values given as output for each sequence from both algorithms concerning their net charge, amphipathicity, hydrophobicity, hydrophilicity and the overall ratio. Indeed, peptides with more positive net charge and more balanced hydrophobicity ratio will most likely have a more positive prediction score regarding their anticancer potential.

Some peptides from different organisms revealed a higher natural anticancer potential score in AntiCP algorithm when comparing their scores against the score of CT-p26. Some examples are the sequences from *Kangiella sediminilitoris* KCTC 23892 and *Xanthomonas euvesicatoria* LMG 933 (0.87 and 0.82 respectively). However these values were still not significant enough to justify a change of study object given that all past works were performed with azurin from *Pseudomonas aeruginosa*.

In Table 2 we can also observe the modifications that AntiCP suggests that increase the overall anticancer potential score based on the database information. These improvements are always point residue substitutions and are very similar among the sequences given their highly conserved level, improving CT-p26 score to 0.85.

All in all, CT-p26 demonstrated putative anticancer potential *in vitro* and the *in silico* study performed by both algorithms defended that this sequence has anticancer potential.

4.2.2. Improvement of CT-p26

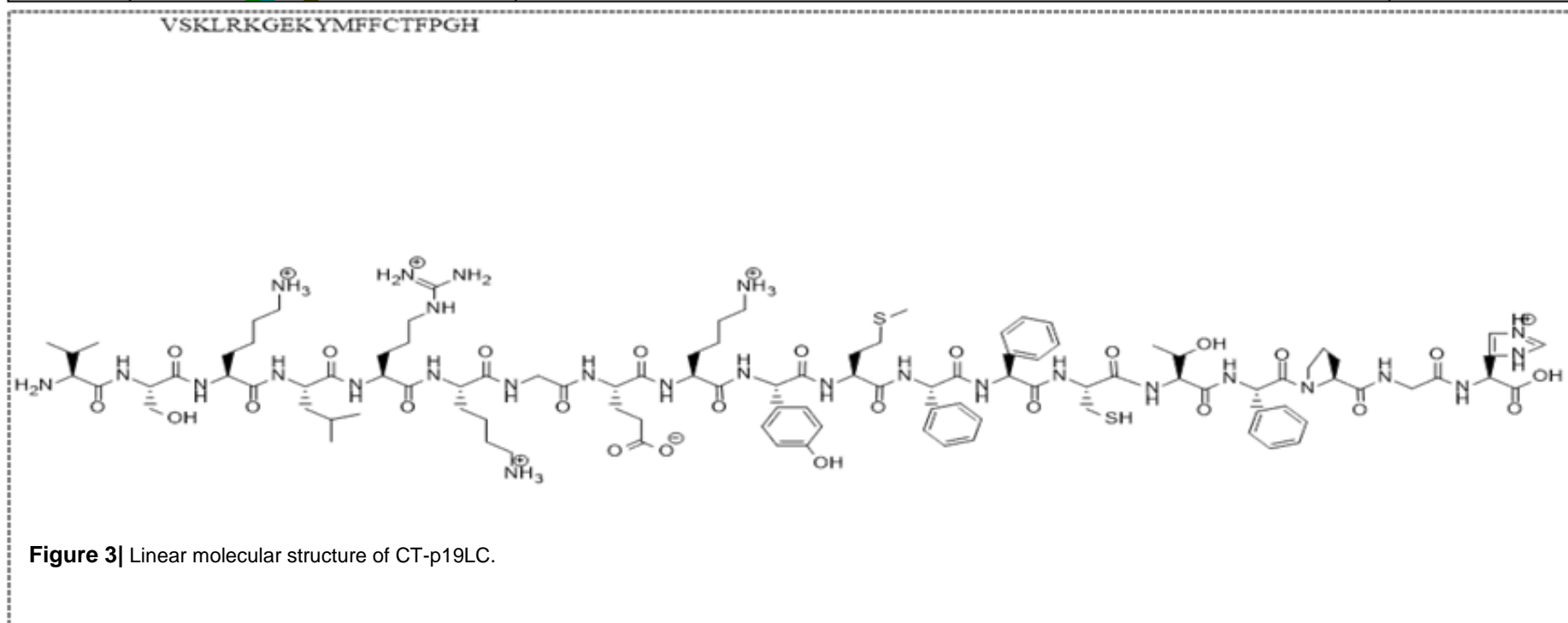
To continue this *in silico* study we aimed for the improvement of CT-p26 with three objectives: increase its anticancer score, shortage of its length and improve its solubility.

In studies which aimed to validate AntiCP algorithm, the peptides with score above 0.90 proved to have anticancer effect *in vitro* and a peptide with score below 0.50 proved to be non-effective (Ghandehari et al. 2015). To our knowledge, besides the tests we performed on CT-p26, no other peptides with scores of specifically 0.76 were previously tested to validate this threshold, so for the further improvement of CT-p26 anticancer potential along with its shortage we decided to aim for values above 0.90, like the references suggest.

Regarding the length change, shortage of sequence in peptides means the decrease of synthesis cost and the increase in the likelihood of reaching its targets within the organisms, as it is suggested that shorter peptides show more anticancer potential and improved selectivity (Harris et al. 2011; Gaspar et al. 2013). Also, as it was demonstrated by previous works on cecropins, it is standard to select the most active parts of proteins or peptides in order to chop dispensable residues or portions that can be disturbing the intended biophysical conformation, essential to create cancer cell membrane pores (Srisailam et al. 2001). The bioinformatic tool AntiCP was once again operated, this time in order to test the anticancer potential in shorter versions of CT-p26. The principle used was to progressively reduce the number of residues only in the extremities of the sequence until an optimal sequence was attained (with better score, net charge and amphipathicity values). Indeed, a series of modifications were tested and its anticancer potential calculated by the algorithm (Table 3).

Table 3 | Summarized list of AntiCP prediction results for different improved versions of CT-p26 until final improvement version, CT-p19LC. Residue substitutions are highlighted.

	Input sequence	Anti-CP						Innovagen	
		Score	Hydrophobicity	Hydropathicity	Amphipathicity	Hydrophilicity	Charge	pH	Water Solubility
CT-p26	VTFDVS K LKEGEQYMFFCTFP G HSAL	0.76	-0.03	0.07	0.48	-0.28	-0.5	5.3	Poor
↓	VTF K VSKL K KKGEQYMFFCTFP G HSAL	0.85	-0.06	0.03	0.72	-0.28	3.5	8.7	Poor
	VTF K VSKL K KKGEQYMFFCTFP G H	0.88	-0.09	-0.17	0.81	-0.23	3.5	10	Poor
	VTF K VSK K KKGEQYMFFCTFP G H	0.93	-0.16	-0.50	0.97	-0.02	4.5	10	Good
	K VSKL K KKGEQYMFFCTFP G H	0.66	-0.15	0.51	0.93	-0.22	3.5	10	Good
	K VSKL K KKGE K YMFFCTFP G H	0.81	-0.17	-0.53	1.00	0.10	4.5	10	Good
CT-p19	VSKLKEGEQYMFFCTFP G H	0.90	-0.08	-0.31	0.66	-0.20	0.5	7	Poor
▼	VSKL K KE K GE K YMFFCTFP G H	0.86	-0.13	-0.35	0.92	-0.05	3.5	10	Good
CT-p19LC	VSKL R KKGE K YMFFCTFP G H	0.99	-0.16	-0.38	0.85	-0.05	3.5	10	Good



The first modification was the removal of the last three residues S-A-L. Alanine and serine are poor hydrophobic amino acids and so their removal was likely to improve hydrophobicity ratio. Also, some dissimilarity in those last residues among the whole sample was observed in Table 2, although no specific pattern was found. That region appears to be very poorly conserved amongst the different species, even within the *Pseudomonas* genus thus was logical that the depletion of this region would arise as first option. Indeed, observing Table 3 is possible to conclude that the removal of the last three residues improved the anticancer potential score of this peptide calculated by AntiCP from 0.85 to 0.88.

Preliminary tests in CT-p26 showed that this peptide had solubility issues when using PBS as solvent. This is a normal consequence of peptides with positive or next to positive net charge. Because the hydrophobic nature of residues confers its overall net charge and influence other characteristics such as pH, the issue that this new improved peptide would not be easily soluble ascended. *In silico* approaches using solubility prediction algorithms were used to forecast this problem. Innovagen™ website has a peptide solubility calculator which upon the use of the peptide sequence as input will provide as output the water solubility, pH and, if poorly soluble, solvent alternatives. Innovagen™ peptide calculator makes calculations and estimations on physicochemical properties such as peptide molecular weight, peptide extinction coefficient, peptide net charge at physiological pH and peptide iso-electric point.

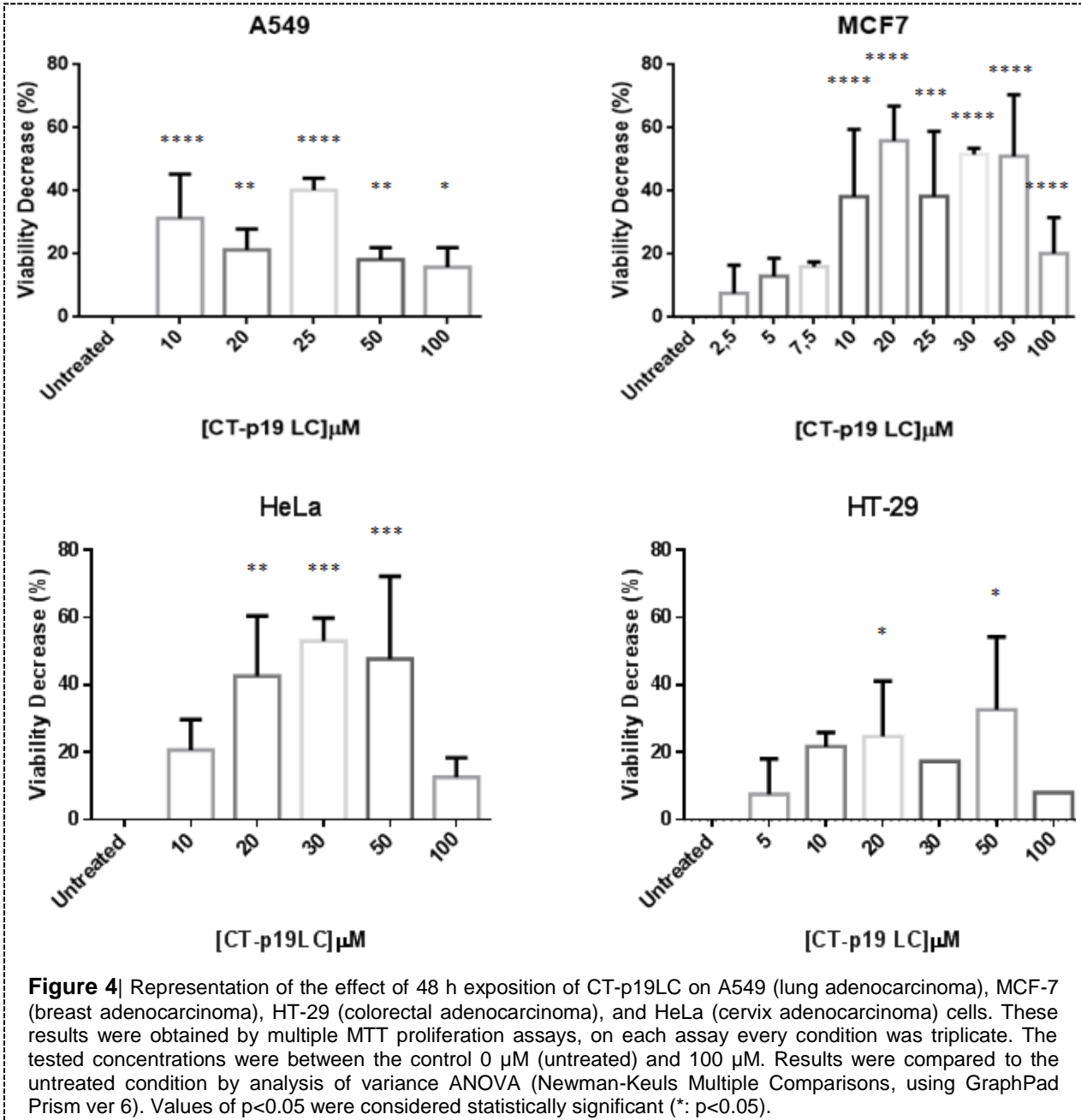
Consequently, in Table 3 is also possible to observe if the tested sequences in AntiCP have poor or good water solubility despite their anticancer potential score. Indeed, the depletion of the three last residues increased its hydrophobicity ratio but did not improve its poor solubility. Nevertheless, we also tested the CT-p26 sequence with minus seven residues (CT-p19) by depleting the first four residues as well, even though they were hydrophobic ones and an optimal score of 0.90 was given as output.

Finally, with the suggested single substitutions given by the algorithm, anti-CP's score increased to 0.99 and the solubility prediction improved. As a consequence, a new putative peptide with anticancer potential was designed using CT-p26 as template, a peptide derived from *P. aeruginosa*'s azurin. As introduced, the designation given was CT-p19LC, because it has 19 residues instead of 26 and the original template comes from the C-terminal extremity of azurin. The CT-p19LC chemical linear structure and sequence can be observed in Table 3 and Figure 3.

4.3. Cytotoxic effect of newly designed CT-p19LC on cancer cells

After CT-p19LC synthesis, MTT proliferation assays were performed to access the effect of this newly designed peptide on cells of lung adenocarcinoma line (A549), breast adenocarcinoma line (MCF-7), colorectal adenocarcinoma line (HT-29) and cervix adenocarcinoma line (HeLa).

Different peptide concentrations were tested. Given that the maximum concentration usually studied of azurin and p28 is 100 μM , this concentration was the maximum experimented. Cells untreated represent control. The results can be observed on Figure 4 bellow.



When preparing the recently synthesized CT-p19LC, its good solubility capacity in phosphate buffers was immediately distinct confirming Innovagen's algorithm prediction. Although the prediction was water based, this buffer has close-to-neutral pH.

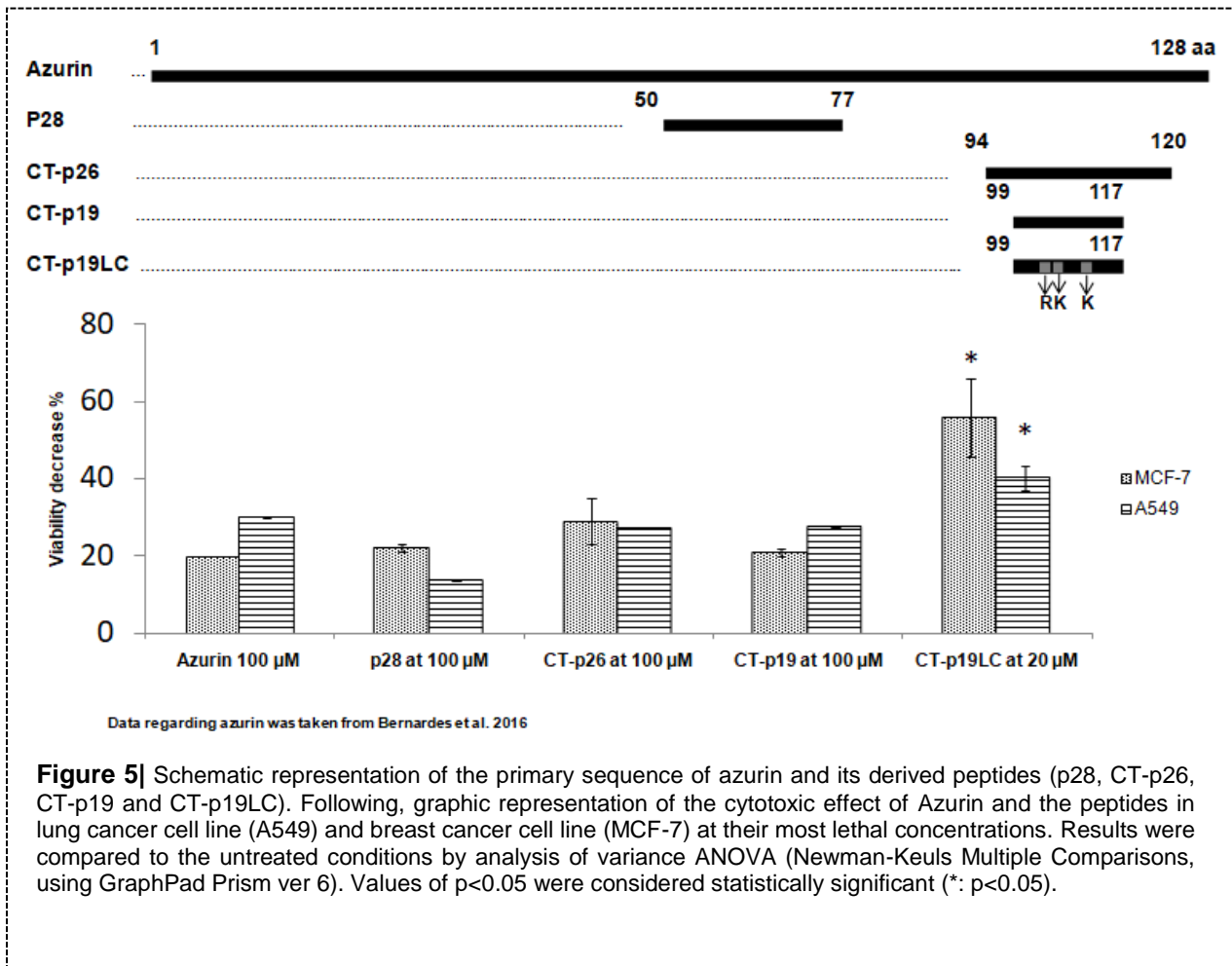
In Figure 4, CT-p19LC reveals to be active against all tested adenocarcinoma cell lines, although, instead of a dose depended behavior, what it seems to be a bell-shaped biphasic cytotoxic behavior is observed. Such behavior was described on other anticancer agents who induce targeted necrosis in cancer cells or related with anti-angiogenic agents (Reynolds 2010; Wong et al. 2015). This result does not add up to the already known dose dependent profile which trends in azurin, p28 and CT-p26 cytotoxic assays, which is impressive considering that CT-p26 is the template of CT-p19LC.

Indeed, in the assays using CT-p26, p28 and reportedly azurin itself (Bernardes et al. 2017 submitted) cell viability decreased upon gradual dose concentration upgrade which leads to the conclusion that the cytotoxicity power of those peptides appear to trigger a dose depended behavior. Also, on CT-p26 and p28 cell viability profiles, cell death seems to stabilize in concentrations near 50 μM (Figure_S2). In the same conditions, reports of p28 assays confirm the dose dependent cytotoxicity against malignant cells (Yamada et al. 2013). Consequently, both assays in p28 and CT-p26 in MCF-7 demonstrated a very similar cytotoxic profile (Figure_S2).

Adding to improved solubility and despite the different cytotoxic profile, CT-p19LC indeed seems to have an improved anticancer potential. There seems to be a maximum viability decrease on human breast MCF-7 cells which never exceed 30% with high peptide doses (100 μM) when treated with CT-p26 or p28 (Figure 5). Yet, the average lethal dose of CT-p19LC appears to be much lower. With CT-p19LC concentrations near 20 μM , a fifth of the concentrations with maximum effect when using the other peptides, MCF-7 cells registered a viability decrease of about 60%, which represents what appears to be an improvement of effectiveness by 2-fold in comparison with the template peptide and azurin itself. These results suggest that azurin's anticancer potential is not limited to p28 fragment substantiating the hypothesis that the residues near azurin's C-terminal that compose CT-p26 may also lethally target cancer cells, in an effective way. Given that this peptide is originated from a tridimensional zone of azurin with high hydrophobic power which is very relevant for azurin's membrane targeting capacity we can also add that the results shown in both Figure 4 and Figure 5 may suggest a possible improvement in the membrane targeting capacity of CT-p26 and azurin converted in CT-p19LC. All in all, *in vitro* assays results show that CT-p19LC represents an improved version of its model CT-p26, validating the algorithm predictions of optimization in anticancer targeting when tested in breast cancer cell line MCF-7.

The same degree of apparent anticancer effectiveness was observed in assays performed on human (A549) lung adenocarcinoma cells (Figure 4). With only 25 μM of CT-p19LC lung cell viability decreased more than 40%, which represents 10 to 15% more cell death than the maximum viability decrease caused by azurin and CT-p26 in A549 cells, and still these data is a representation of concentrations such as 50 and 100 μM , two and four times the concentration used for treatment with CT-p19LC (Figure 5).

In fact, in Figure 5 it is possible to observe that the activity against breast MCF-7 cancer cells of CT-p19LC improved at least 2-fold in comparison with the azurin's and p28's effect when used in less concentration (20 μ M). The same appears to happen upon treatment of A549 cell line with CT-p19LC which appears to kill 2-fold more lung adenocarcinoma cells than p28. This represents a very significant result given that p28 already passed two clinical trials on patients with advanced and recurrent solid tumors, extending life expectancy of at least three patients with metastatic cancer, including in the lungs (NCT 00914914).



On another subject, the implications of the biphasic profile observed in all cell line assays upon treatment with CT-p19LC represent an interesting outline of these assays. The propositions of these results are only possible to discuss based on the little information that is offered in literature with significant proof of the advantages and/or disadvantages of this pharmacological behavior.

In one hand is possible that this apparent biphasic behavior may represent a step back for the anticancer potential of this molecule given that up until very recently the pharmacokinetics of anticancer agents were calculated only based on maximum tolerated dose. The need to calculate effective drug

usage considering any other type of behavior other than dose-dependent can still be enough to condemn any new potential anticancer drug in face of risk assessment of the drug regulatory authorities (Calabrese 2004). Indeed, from some time, cancer patients have been regularly treated with chemotherapy drugs at the maximum tolerated dose. According to the threshold dose-response model, this should maximize the chance of eradicating all tumor cells and succumb to the best therapeutic index.

In another hand, some defend that a biphasic profile is not anything but the true profile for the general drugs and that a maximum concentration of effectiveness is not necessarily the highest tolerable. Consequently, instead the dose-response to many drugs may be preferentially modeled using 'hormetic' or 'biphasic' dose-response models (Reynolds 2010). Hormesis can manifest in several forms: bell-shaped, U-shaped or J-shaped dose-response curves. A bell-shaped dose-response is characterized by low-dose stimulation, followed by loss of this effect at higher doses, as observed Figure 4 with all assays performed on breast, lung, colorectal and cervix adenocarcinoma cell lines. The CT-p19LC effect on these cell lines assumes a bell-shape dose-response where in lower doses CT-p19LC is very bioactive and in higher doses its effect decreases.

Nevertheless, CT-p19LC suffered three point residue alterations and was reduced hence increasing its hydrophobicity. Peptides secondary structures are highly dynamic and easily triggered. Therefore is very possible that by trying to improve membranolytic effect of CT-p26 therefore creating CT-p19LC an alteration on the preferable secondary structures adopted by this peptide occurred.

As such, future re-design of this peptide may be needed if biphasic behavior proves difficult to handle or to extend to more cancer cell lines.

On Figure 4 it is also possible to analyze the assays performed on HeLa (cervix adenocarcinoma) and HT-29 (colorectal adenocarcinoma) cell lines. Although the results of assays performed on HeLa cells resemble the ones already discussed about CT-p19LC effect on A549 and MCF-7, the same does not happen when analyzing HT-29 results. The average LD₅₀ of CT-p19LC increases from 20 to approximately 50 μ M when compared with results of assays performed on breast and lung cancer cells. The maximum cell viability decrease values were reported to be more than 60% on HeLa cells treated with 50 μ M of CT-p19LC and 40% on HT-29 cells treated with CT-p19LC. These results suggest that HT-29 cells are somehow more resistant to CT-p19LC than MCF-7, A549 and even HeLa cells. Although it is supposed that CT-p19LC mode of action is membrane based its targets may be dissimilar in different types of cancer cells. These differences between cancer cell lines may be the key to unravel this peptide target against human cells. It has been suggested in another work from this group that azurin's 114 residue is important on targeting caveolin (Bernardes et al. 2017 submitted). The peptide CT-p19LC is designed from that same region containing that same residue which imposes that a putative CT-p19LC interaction with caveolin-1 should be studied in the future. Indeed, it is known that caveolin-1 expression levels differ from cell to cell, and there is no *caveolae* model associated with all cancer cells which means that even within the group of epithelial cancers there may be variances in the caveolin-1 expression pattern (Martinez-outschoorn et al. 2015). In an attempt to get some clues about a possible interaction of CT-p19LC with caveolin-1 we verified by western blot analysis that HT-29 cells' caveolin-1 content is very

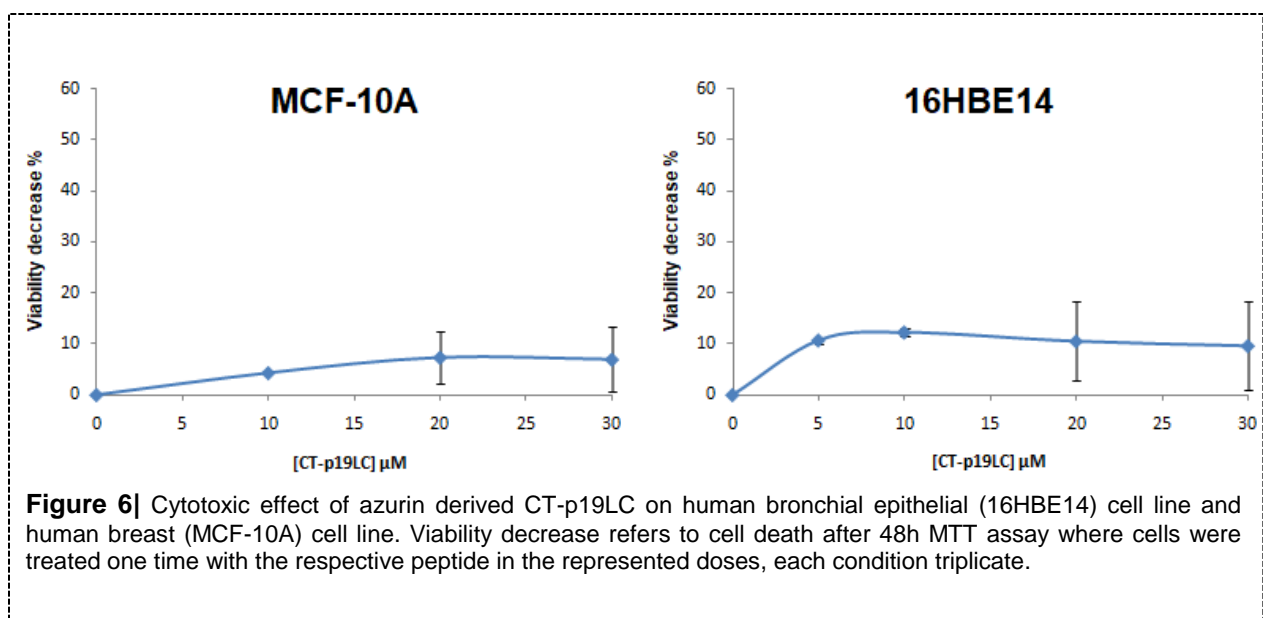
low indeed (Figure_S1). Although this result does not allow a significant conclusion about CT-p19LC mode of action and does not answer the question about the different cytotoxic effect we observe in the different cell lines it represents an indication about how dissimilar the membrane's content of cancerous cells are among the different types of cancers. Indeed, if CT-p19LC interacts with the lipid rafts of cancer cells then caveolin-1 may be a candidate, but probably not the only one.

4.4. CT-p19LC is not effective against breast and lung non-cancer cell lines

After confirming the existence of apparent improved activity of CT-p19LC against breast, lung, colorectal and cervix adenocarcinoma cells, it seemed important to assess if this peptide was toxic against non-cancer cell lines resultant from similar tissues.

In order to test if CT-p19LC shows immediate toxicity against non-cancer cells, two non-malignant cell lines from human lung (16HBE14, bronchial) and from breast (MCF-10A) were treated with different doses of CT-p19LC following an MTT assay to unravel cell proliferation levels (Figure 6). Given that the LD₅₀ of CT-p19LC calculated in the assays performed on both A549 and MCF-7 (Figure 4) were the same, around 20 μ M, it seemed important to study the effect of that same concentration on the non-cancer cell lines from the same type of tissue.

This preliminary analysis on CT-p19LC effect on non-malignant cells showed very promising results (Figure 6). Despite the apparent cytotoxic effect against the lung cancer cell line A549, assays on normal lung cells registered little toxicity when treated with CT-p19LC, attaining less than 15% of cell viability decrease. The same happened in the assay performed on breast cancer cell line MCF-10A. Less than 10% of cells lost their viability, which is not considered a significant cytotoxic effect.



Comparing these results to those obtained with the cancer cells some important implications can be considered. The peptide CT-p19LC decreased cell viability by 60% on MCF-7 breast cancer cells (Figure 4) with only one dose of 20 μ M whereas the same amount of peptide killed less than 10% non-cancerous breast cells (MCF-10A), a reduction of more than 50% on lethality. This result suggests that this peptide somehow kills preferentially breast cancer cells instead of non-cancer ones. The same was observed in the assay performed on non-malignant lung cells from human bronchial tissue (16HBE14) in comparison with the previous assays on A549 cell line, lung cancer cells. Cancer cells viability decreased by 40% with a single 20 μ M dose of CT-p19LC whereas the same amount of peptide only seem to kill 10% of all non-cancerous 16HBE14 lung cells. Again, CT-p19LC bioactivity seems to include what appears to be specificity toward cancer lung cells in comparison with cells derived from normal tissue.

Specificity toward mammalian cancer cells is not new when discussing anticancer peptides. In fact, the characters of high hydrophobicity and overall positive net charge are linked to the capacity of ACP_{AO} exclusively targeting cancer cells and being non toxic to normal cells. The biophysics related to this phenomenon is associated with cancer cells' membrane composition which is different from non-cancer cells membranes. Cancer cells' membranes have an overall negative net charge on the outer leaflet given its high composition in certain phospholipids such as PS (Teixeira et al. 2012). The *in silico* improvement of CT-p26 into CT-p19LC performed in this thesis project had a focus on the two biophysical characters above mentioned: hydrophobicity and net charge, besides length shortage.

Thus, this preliminary result suggests that we may be in the presence of an ACP_{AO}, although more repetitions and extension to more non-cancerous cell lines should be performed in the future.

4.5. CT-p19LC decreases the membrane order of cancer cell lines

Up until now all tests and data suggest that not only the newly designed peptide CT-p19LC appears to have anticancer potential but that such potential seem to surpass the cytotoxic capacity of its template peptide and even azurin and p28 in at least two cancer cell lines: lung (A549) and breast (MCF-7). It has also been suggested that CT-p19LC has the capacity of specifically target lung and breast cancer cells given its lack of significant lethality on assays performed on non-malignant cancer cell lines from the same type of tissues. Although these abilities have been reported on other peptides they are considered quite appealing and have been objective of many studies.

The important questions asked more frequently are what are ACP_{AO} (the specific type of anticancer peptides that do not target mammalian healthy cells) mode of targeting cancer cells and on which cancer cell section or internal compartments do they operate against. As introduced before, the majority of action happens on the membrane basis. Simultaneously, these peptides use some membrane components such as PS to target cancer cells and act against them. Their biophysical conformation alongside their hydrophobic nature creates the necessary conditions for them to attach and penetrate cancer cells. Also,

membrane-active anticancer peptides are known to present several mechanisms of action, including “barrel-stave” mechanism, “carpet” mechanism, “toroidal pore” mechanism and “disordered toroidal pore” mechanism (Nguyen et al. 2011).

In addition, azurin is also suggested to enter cancer cells. A process of targeting and disrupting *caveolae* and remove from the cell membrane selective receptors that may be over active is suggested to take place (Bernardes et al. 2014). Previous results from our group showed that azurin enters cells through endocytosis mediated by *caveolae* and has an impact on the cell lipid rafts organization that is very similar to the impact caused by M β CD (Methyl- β -Cyclodextrins), an agent that can disrupt lipid rafts by removing cholesterol from the membrane (Sanchez et al. 2011).

Therefore, it would be significant to verify the effects of CT-p19LC at the level of the membrane order. To do so, the order of the plasma membranes after treatment with the CT-p19LC peptide was investigated with the probe Laurdan using confocal microscopy in lung (A549), breast (MCF-7), colorectal (HT-29) and cervix (HeLa) adenocarcinoma cell lines. Consequently these cells were treated only with 20 μ M which is the concentration of CT-p19LC we consider had the major impact in the MTT assays (Figure 4).

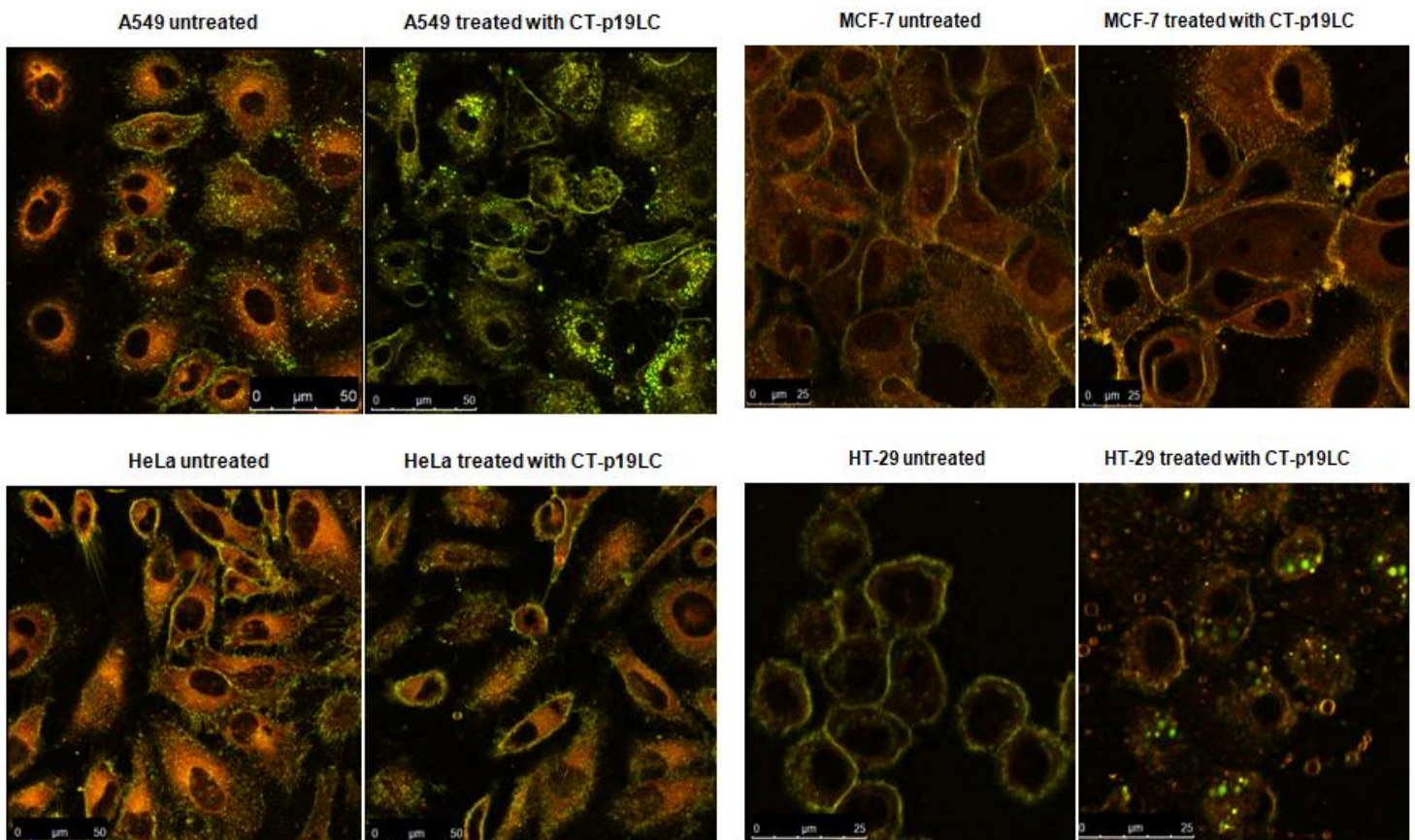


Figure 7 | Impact of CT-p19 on the membrane fluidity of cancer cell lines MCF-7, A549, HeLa and HT-29. Cells were loaded with 5 μ M of Laurdan after incubation with 20 μ M of peptide for 2 hours. Laurdan GP values were determined as described in Material and Methods.

Confocal microscopy images showed that treated cells from all cell lines suffered a variety of morphological modifications. The cell shape became irregular and the fragmentation of the plasmatic membrane and the nucleus was visible (Figure 7).

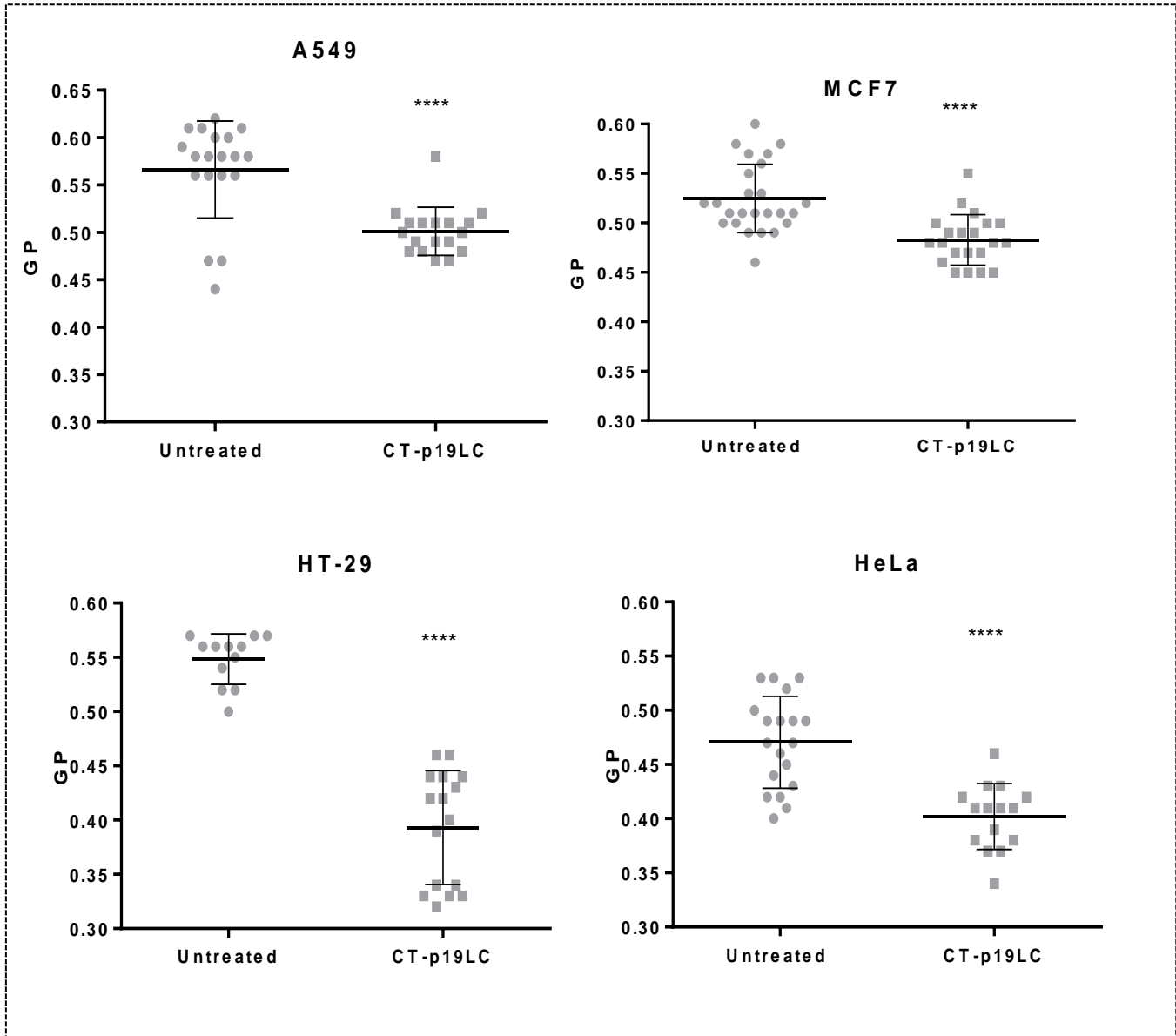


Figure 8| The effects of CT-p19LC in the cell's membrane order of A549 lung cancer cell line, MCF-7 breast cancer cell line, HT-29 colorectal cancer cell line and HeLa cervix cell line and their respective GP values. All represented cell lines were seeded on μ -Slide glass 8 well glass bottom chambers and treated with 20 μ M of CT-p19LC for 2h. For each condition 5 μ M of Laurdan were used. Untreated cells were the control. Software based on a MATLAB environment was used to measure the GP values. Average GP values are expressed as mean \pm SD from at least 15 individual cells in each condition. Results were compared to the untreated by student's t-test two tailed distribution two sample equal variance (****: $p < 0,0001$).

However, to be sure what are the real differences between the high and low ordered contents in the cells, the degree of lipid packing had to be measured. In order to quantify the degree of lipid packing (GP value) in all cell lines and in both conditions (untreated and treated with 20 μ M of CT-p19LC), a software based on a MATLAB environment was used (provided by Dr Fábio Fernandes, CQFM, IN).

The GP value varies between -1 and 1, and higher the value the higher is the ordered content of the cells. A $GP \geq 0.5$ tells us that we are in the presence of a gel phase, in other words a $GP \geq 0.5$ correspond to a very compact and ordered content. Below that level, we are in the presence of a more fluid phase (Owen et al. 2011; Pinto et al. 2013).

As we can see in Figure 8, untreated A549 cells have an average GP of 0,56, meaning that these cells' membranes are considered ordered. When A549 cells were treated with CT-p19LC, a significant decrease in the GP value (0.56 to 0.51) was observed when compared with the untreated cells, meaning that the ordered content of the cells decreases after CT-p19LC treatment. The same pattern is observed in the tests performed on the other cell lines. Untreated MCF-7 breast cancer cells have an average GP of 0,53 which means the membranes are in the gel phase but upon treatment with CT-p19LC average GP decreases to 0,48, a value which indicates the membranes are in the fluid phase.

The peptide CT-p19LC has decreased GP average of cervix cancer cells (HeLa) from 0,48 to 0,40. These results suggest that these cells do not have a high content of ordered domains in their structure. There is no pattern among cancer cells related to their *caveolae* levels, even within the adenocarcinoma types there are variations regarding membrane fluidity and lipid rafts (Martinez-outschoorn et al. 2015). Nevertheless, when we treated HeLa cells with CT-p19LC, the GP obtained was 0.40. Like the other cancer cells' results, a decrease in the ordered domains was observed after CT-p19LC treatment, meaning that this peptide appear to able to decrease the ordered domains of all these adenocarcinoma cell lines. (Singh et al. 2003; Pang et al. 2004)

The most drastic effect observed in cell membrane order with this methodology was when treating HT-29 colorectal cancer cells with CT-p19LC. Untreated cells have an average GP of 0,55, a value that suggests the membrane components are ordered and compact but upon treatment with CT-p19LC for only two hours this value decreased to 0.40 which means the membranes of these cancer cells became very fluid. This result seems to be in conflict with MTT assay results presented on Figure 4, where HT-29 appeared to be slightly more resistant to CT-p19LC in contrast with the other adenocarcinoma cell lines. However, we do not still fully understand CT-p19LC action and although its design and preliminary cytotoxic results may lead to the assumption that we are in the presence of a membranolytic peptide, we still do not know which components this peptide targets. For now, the GP results might indicate that CT-p19LC interacts in some way with lipid rafts but as introduced there are different types of lipid rafts, more specifically there are non-planar lipid rafts and planar lipid rafts. In fact, HT-29 cells are more prone to form planar lipid rafts in contrast with the other adenocarcinoma cell lines in study, which are richer in non-planar lipid rafts.

Even though membrane order assay using Laurdan's probe is not a standard approach to study membrane-active anticancer peptides mode of action, it revealed very significant data regarding the level of effect this peptide had on these cancer cells' membranes. However, information regarding the specific target within the plasmatic membrane and mode of entry still lacks. Usually, studies that aim to unravel the targets of lytic anticancer peptides in cancer cell's membranes are performed using a tryptophan residue within the peptide as a fluorescent probe to study its behavior. Using this approach it is possible to demonstrate their modes of selection and pore-formation fashion (Li et al. 2014).

Accordingly, in the literature there is also data regarding the biophysical changes on membranes caused by anticancer peptides and even azurin disposed by Atomic Force Microscopy. In 2016, Bernardes et al. demonstrated that azurin administration leads to changes in biophysical properties of the plasma membrane of cancer cells, thereby causing changes in signaling pathways that mediate drug resistance. These effects may be of particular interest in drug resistant cancers, where the more rigid nature of the membrane was associated to increased resistance to the accumulation of anticancer drugs. Therefore, since azurin may disrupt lipid rafts, the effects of co-administrated drugs are enhanced (Bernardes et al. 2016). Another example was the tests performed on anticancer peptide HNP-1. AFM data suggested that HNP-1 was more active against solid cancer instead of hematological ones because of differences on membrane resistance and rigidity between two different cell lines, one of prostate carcinoma, a solid tumor and other from a type of lymphoblastic leukemia, a hematological tumor. Also, using AFM it was possible to confirm that, although HNP-1 appears to be membrane-active, the cancer cell's final collapse is due apoptosis (Gaspar et al. 2015).

In fact, even though, CT-p19LC was designed to have high hydrophobicity and positive net charge that indicate it is more prone to target cancer cells' membranes instead of the non-malignant ones, there is no proof about its mode of action. This membrane order assay reveals that these four adenocarcinoma cell's membranes are highly disturbed upon CT-p19LC treatment in very small doses (20 μ M) for a very short time (2 h) which may lead to the conclusion that this peptide's target it is in fact part of these cells membranes adding that lipid rafts constituents are good candidates, including caveolin-1. But the mode of action regarding what caused these cells lethality levels observed in Figure 4 still remains a mystery and may or may not be related to the plasmatic membrane given that internal processes are also a possibility such as apoptosis. For future studies, other biophysical approaches such as AFM or leakage studies using model membranes (liposomes) would be significant to unravel CT-p19LC mode of action against cancer cells.

4.6. Treatment with CT-p19LC in combination with erlotinib potentiates the anticancer effect of this agent in lung cancer cell line A549

It has been demonstrated in previous studies that azurin, CT-p19LC protein of origin, and p28, have a strong enhancer anticancer effect on cancer cells when they are used along with chemotherapeutic drugs (Bernardes et al. 2016; Yamada et al. 2016). Erlotinib is a chemotherapeutic agent which targets EGFR. This receptor is of major relevance in lung cancer therapy. In order to invade the surrounding tissues, tumor cells need to adhere to the extracellular matrix (ECM). These events of cell adhesion are possible due to the presence of cell-surface receptors such as the integrin superfamily. Integrins are able to promote the intracellular signaling of other membrane proteins such as Growth Factor (GF) receptors. It has been recently demonstrated that in lung cancer cells β 1 integrin controls Epidermal Growth Factor receptor (EGFR) signaling and tumorigenic properties suggesting that this transmembrane protein may be a suitable target for therapies (Howe et al. 2016).

Given the fact that CT-p19LC is derived from azurin and that the effect of this peptide on A549 lung cancer cells appears to be higher than azurin's effect (Figure 5) it was relevant to study the possibility of synergy between CT-p19LC and erlotinib upon exposure on this cell line. This synergy phenomenon is when the effect of the drugs combined is higher than the arithmetic sum of their solo effect (Preet et al. 2015).

The human adenocarcinoma lung cancer cells A549 were seeded in 96-well plates and in the next day, these were exposed to 10 and 20 μ M of CT-p19LC together with 0.5 and 1 μ M of erlotinib during 72 hours. Untreated cells or cells treated with each agent alone were used as control, in order to determine the relative cell viability of treated cells. For these studies, drugs were added in concentrations close to their LD₂₀ and LD₅₀ (Figure_S3). In Figure 9, results suggest that CT-p19LC may influence the effect of the drug treatment in cell death. The solo effect of CT-p19LC at concentration of 10 μ M was a decrease in cell viability in about 25% (blue), which is consistent with results of MTT assays represented in Figure 4. The solo effect of erlotinib at concentration of 0.5 μ M was a decrease in cell viability in less than 10% (yellow), which is consistent with erlotinib standard lethality values and usually represents less than LD₂₀ (Figure_S1).

When treating A549 cells with both drugs, if no synergy occurred it was expected that the effect was a viability decrease of 35% or less, however, a viability decrease of almost 50% was observed, which represents an upgrade of 15-20% on drug effect (red). This result strongly suggests that CT-p19LC enhances erlotinib effect. Collectively, both drugs in small doses (LD₂₀ or less) upgrade effects reaching a LD₅₀ concentration.

Synergy is also observed in results from joint treatment of erlotinib at concentration of 0.5 μ M with CT-p19LC at concentration of 20 μ M, although not so evident (Figure 9).

When combining erlotinib at concentration of 1 μ M with CT-p19LC, higher activity levels than individual cytotoxicity is observed but no potentiating is suggested given the fact that viability decrease

levels of the combined treatment were not superior to the sum of the individual cytotoxic levels. Overall, it is to note that when CT-p19LC is present, there is an increase in the levels of cell death in comparison to the viability decrease levels observed when erlotinib is added alone at concentration of 0.5 μM .

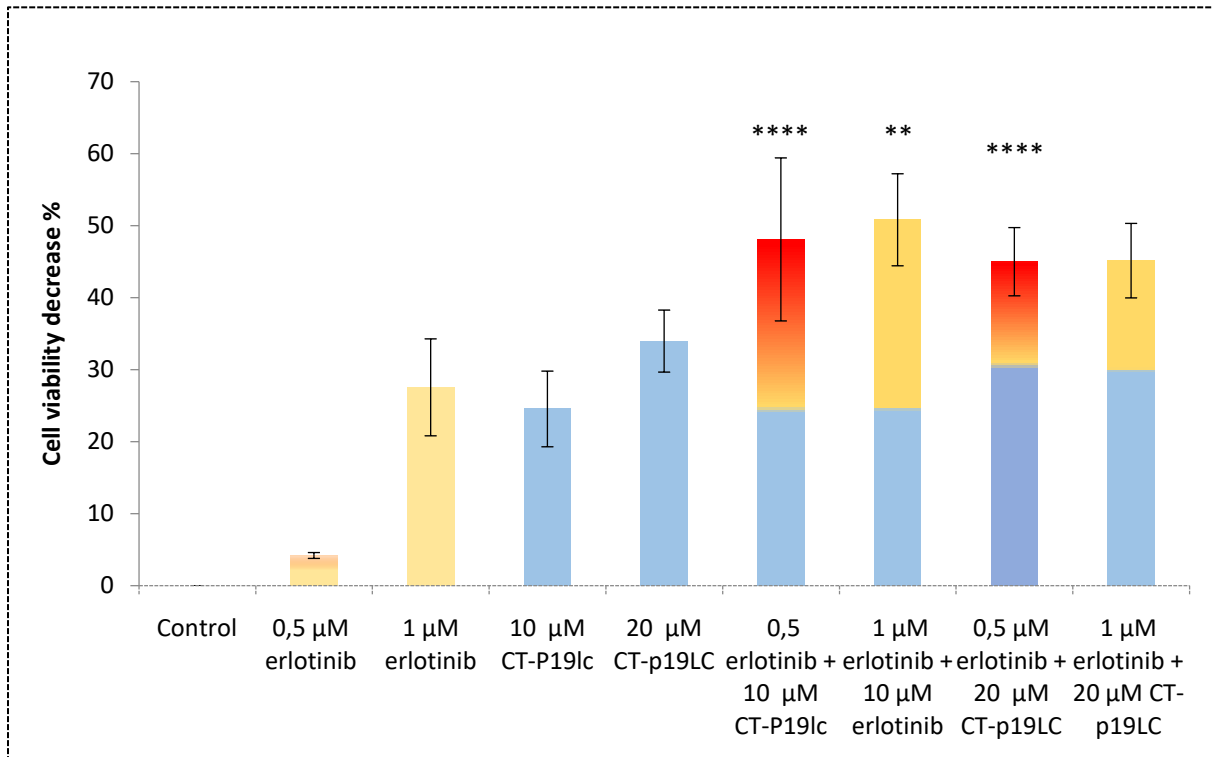


Figure 9| CT-p19LC potentiates the effects of erlotinib. Cells were seeded at a density of 4×10^3 A549 cells per well was performed in 96-well plates and left to adhere overnight. In the next day, cells were treated CT-p19LC (10 μM and 20 μM), erlotinib (0,5 μM and 1 μM) or a combination of both. After 72h, cell proliferation was determined by MTT assay. Results are expressed as percentage of cell death relative to the control (untreated cells). Values of A549 cell viability decrease are presented as mean + SD. Yellow represents effect of erlotinib only, blue represents effect of CT-p19LC only, and red represents the percentage of viability decrease which goes beyond the sum of the effects of CT-p19LC and erlotinib combined. Results were compared to erlotinib's solo values by analysis of variance ANOVA using GraphPad Prism (ver 6). (**: $p < 0,01$).

A possible hypothesis to explain this synergistic effect could be that CT-p19LC, similarly to azurin, affects, at least in part, the signaling pathways related to *caveolae* and EGFR which is targeted by erlotinib.

Previous results (Bernardes *et al.* 2017, submitted) suggests that azurin enhance paclitaxel and doxorubicin cytotoxic effect on MCF-7, HT-29 and A549 human cancer cell lines. These results were acquired after these adenocarcinoma cells were exposed to 25, 50 and 100 μM of azurin together with 0.1, 1 and 10nM of paclitaxel or 0.1, 0.5 and 1 μM of doxorubicin during 72 hours. With this study Bernardes *et al.* were capable of observing that the cell death caused by the combination of both drugs was much higher than the cell death caused by the each substance used independently. Another study of our group also revealed that upon exposure of azurin with gefitinib in lung cancer cells A549, there was a higher decrease in β_1 integrin levels in contrast with exposure to either of the agents alone. This result is rather relevant given the fact that the overexpression of β_1 integrin in lung cancer has itself been

associated to the resistance to the treatment with gefitinib, a process that is at least in part mediated by the signaling pathways that are attenuated by azurin. In this study the synergistic effect is evident by an increase of about 15-20% in lung A549 cell death when compared to the sum of the solo cytotoxic effect of azurin and gefitinib. Also, the same result was observed when erlotinib tested in combination with azurin. An identical synergistic behavior was demonstrated by a decrease of 10% in cell viability in comparison with the effect of the single agents, azurin and erlotinib (Bernardes et al. 2016).

The peptide p28 have also been reported to enhance DNA-damaging and antimitotic drugs anticancer effect. In combination with lower concentrations of doxorubicin, dacarbazine, temozolamide, paclitaxel and docetaxel, p28 increased their cytotoxicity by activating tumor-suppressor protein p53, which subsequently induced the endogenous cyclin-dependent kinase inhibitor p21, reducing levels of cdk2, resulting in cell cycle inhibition at G2–M phase and leading to apoptosis (Yamada et al. 2016).

Nevertheless, one may not forget that CT-p19LC is *per se* capable of cell death and membrane disorder as evidence was already presented. Consequently, there may be other possible mechanisms that CT-p19LC may interfere with, not contributing directly to cell death, which may increase the efficiency of other agents.

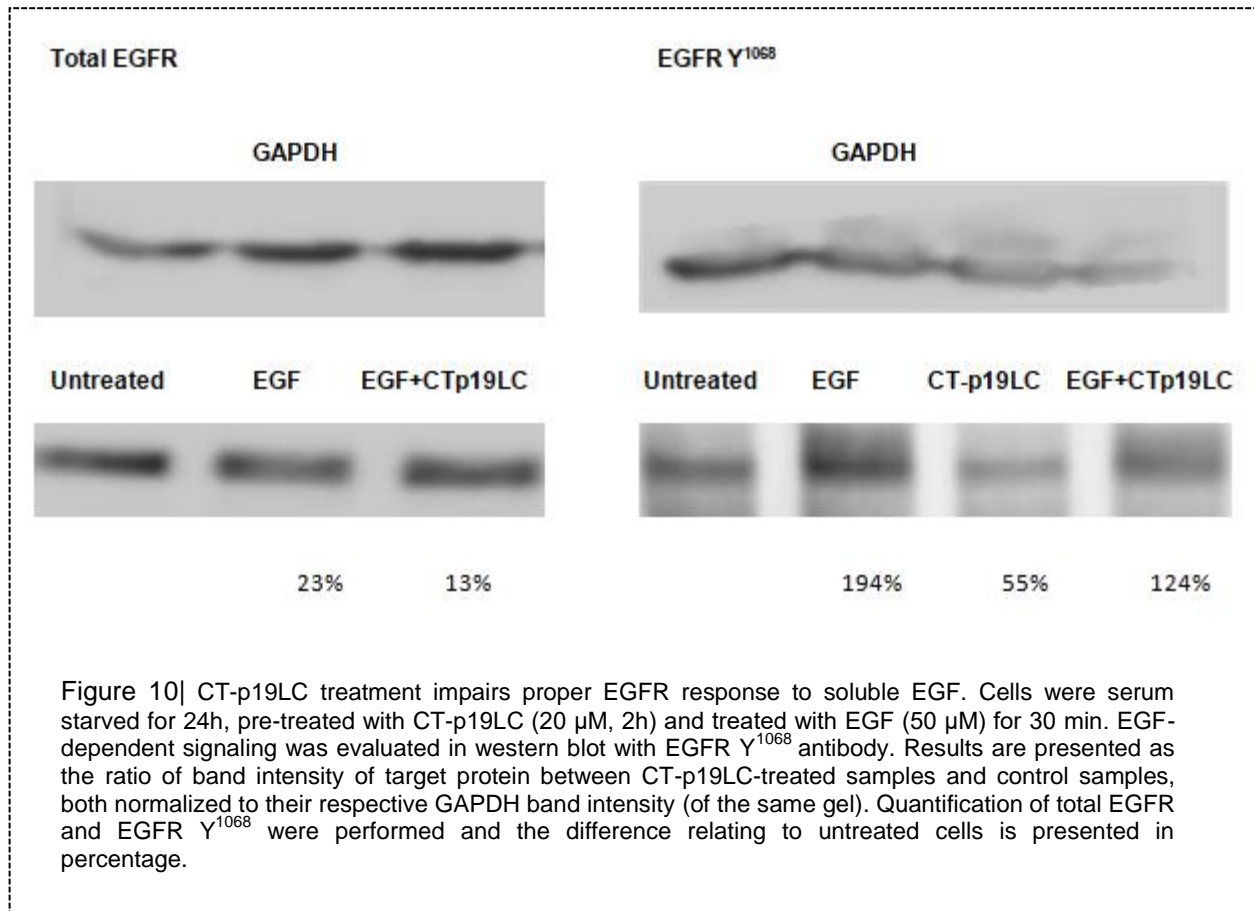
Indeed, it is widely implicit that, although chemotherapy and radiotherapy remain the most common non-surgical cancer treatment options, they present major drawbacks. These include adverse side effects such multidrug resistance. Moreover, these agents can also cause significant cardiotoxicity and neurotoxicity that may force treatment to become dose-limiting (Chu & De Vita 2015). Consequently, it is imperative to develop new therapeutic strategies, more effective in killing cancer cells but also more selective so the toxic side effects associated to administration of anticancer drugs can be attenuated, if not eradicated.

4.7. CT-p19LC perturbs EGF-stimulated trigger of phosphorylated EGFR (Y1068) on A549 lung cancer cells

EGFR is only active in the cells' signalization pathway in its phosphorylated form. Indeed, erlotinib mode of action when targeting EGFR is to enable its phosphorylation to occur. Following the previous results which suggested that CT-p19LC enhances erlotinib effect on A549 lung cancer cells we proceeded to understand if CT-p19LC itself has any effect on EGFR. The signal for EGFR phosphorylation is given by the binding of EGF to EGFR so we tested the ability of CT-p19LC-treated A549 cells to respond to Epidermal Growth Factor (EGF). EGF was added at concentration of 50 μ M in serum-starved cells exposed to CT-p19LC for 2 h or in absence of this peptide, afterwards we proceeded to the protein extraction and western blot analysis to search for total EGFR and phosphorylated EGFR (EGFR Y¹⁰⁶⁸) levels. The results are presented in Figure 10.

What we observed was that in the presence of CT-p19LC, the levels of phosphorylated EGFR by focus on the signaling related residues Y¹⁰⁶⁸ did not increase in the cells exposed to EGF in the presence

of the pre-treatment with CT-p19LC (Figure 10). In contrast, levels of phosphorylated EGFR were higher in cells only exposed to EGF and not to the peptide, which suggests that CT-p19LC has some inhibitory control over the triggering of EGFR, making this signaling pathway a good candidate for the target of CT-p19LC.



5. Conclusions and future perspectives in cancer therapy

Malignant cells are able to provide their own growth signals, ignore growth inhibitory signals, avoid apoptosis, proliferate indefinitely, trigger and sustain angiogenesis and invade tissues through basement membranes and capillary walls. In addition, the dynamics of cancer cell allow them to create resistance mechanisms against the drug paraphernalia used against them (Harris et al. 2011). Thus, cancer therapy active compounds need to be as much, or more, dynamic than tumors themselves. And as a result, it is insufficient to just look for new anticancer agents; it is just as necessary to create new technologies of delivering and enhancing anticancer drugs.

Cancer is predicted to displace cardiac diseases as the principal cause of death globally and its occurrence is estimated to double by the year 2020 and nearly triple by 2030 (Ausbacher et al. 2012).

This disease is instigated by a series of collective genetic and epigenetic changes that occur in normal cells and is characterized by a number of specific, yet very different, behaviors depending on the malignancy type (Harris et al. 2011). The causes can be environmental or genetic, which means that it's modern upraise may be related to peoples' habits and environmental change. Yet, the tumor cells' nature can also evolve and one of the main aspects that can trigger the aggressiveness in this disease is their increasing resistance mechanisms against current anticancer agents. In addition, there is ambiguity and lack of efficiency in the bulk of anticancer agents. The cumulative effect of all these factors is the reason to the alarming cancer burden we hear in the present and for the future.

A great number of studies on anticancer peptides, especially membranolytic peptides, have surfaced in the last decade. Its massive cytotoxicity potential against different types of cancer cells with diverse modes of action in low concentration doses has submitted ACPs as a hot topic amongst the scientific community. Also, their demonstrated effectiveness against multidrug resistant tumors has restored hope in the future of chemotherapy.

At least, five anticancer mechanisms have been proposed for cytotoxic peptides namely cell membrane lysis, inhibition of angiogenesis, activation of extrinsic apoptotic pathways, induction of necrosis, and restoration or action replacement of cell cycle regulator p53. The mechanisms differ in mode of action against both solid and hematological cancers and rare are the peptides that can target and kill cells from both simultaneously.

Although promising, the development of ACPs has its drawbacks. It is pertinent to discuss that the use of peptides in clinical treatments contain both scientific and logistic inconveniences. For instances, poor stability of CAPs (cationic anticancer peptides) in human serum due to the presence of serum proteases can cause peptide degradation and therefore reduce bioavailability (Baxter et al. 2017). It is the case of lactoferricin, a 25 amino acid peptide derived from mammalian source which has shown strong anticancer effect *in vivo* in murines inoculated with lymphoma and melanoma cells. Yet, lactoferricin as an anticancer agent shows some apprehensive limitations given is its susceptibility to enzymatic digestion as well as inactivation by anionic serum components (Harris et al. 2011; Mohd et al. 2015).

The same problem is seen in other ACPs which resemble human peptides since these similarities are not such an extraordinary coincidence. Given that almost all ACPs derive from AMPs and that AMPs, being part of innate immune system, exist in almost all forms of life in a conserved manner, it is not atypical for the human body to have digestion or degradation mechanisms who recognize such peptides.

Nevertheless, anticancer peptides from more distant organisms have been tested and shown promising results. The antimicrobial CS α β -configured defensin from the *Pseudoplectanina nigrella* fungus plectasin displays natural stability in serum. Whilst the bacteriocin plectasin has not been investigated for its anticancer properties, it exhibits promising *in vivo* activity as an antibacterial agent against *Staphylococcus aureus* in combination with other commercial antibiotics (Baxter et al. 2017). Additionally, the microbial-originates azurine-p28 is a success case study of anticancer peptide drug development. The triumph of this peptide is studied to be a result of an improbable combination of a series of favorable factors. Azurin itself is considered a bacteriocin with anticancer potential due to its special biochemical and physical properties.

Consequently, CT-p19LC design and anticancer potential explored in this work may represent a relevant enforcement to the relevance of azurin as an anti-tumorogenic protein. Again, a new portion of this protein was used as template for design of a new synthetic peptide which appears to be cytotoxic against four different adenocarcinoma cell lines. Unlike p28, this peptide suffered three residue modifications from the original template with the goal of enhancing its anticancer potential and gain specificity towards malignant cells through changes in hydrophobicity and net charge. The results from this work suggest that, indeed, CT-p19LC incites higher loss of viability in lung and breast cancer cells in comparison with azurin and p28. It is also bioactive against colorectal and cervix cancer cell lines.

Adding, the results from this work have shown evidence that CT-p19LC, like azurin, has a deleterious effect on membrane order of these four adenocarcinoma cells. Whether this represents an impair effect on caveolae and EGFR on lung cells as it was demonstrated previously from past work of this group to occur when treating these cells with azurin and gefitinib or erlotinib (Bernardes et al. 2016) it remains to be proved. It is also possible that CT-p19LC effect on cancer cells membranes is toxic enough to potentiate the effect of other drugs, such as erlotinib. It would be relevant to study CT-p19LC mode of action in the future. Also, it would be significant to perform more assays to determine CT-p19LC specificity towards more non-cancer cell lines besides human breast and lung cell lines so this peptide specificity properties could be further explored, being one of the most attractive characteristics it seem to present.

Subsequently, anticancer peptide drug development is now substantially depending on drug design software's as demonstrated by the *in silico* workflow followed during this thesis project. These bioinformatic tools allow the improvement or *de novo* construct of potential anticancer peptides by predicting their antitumor competence and are expected to have a more powerful significance in the future of peptide optimization. To complement, during the last 30 years, drug delivery has been one of the fields where peptides have caused a high impact, as proven by the design and development of CPPs (cell penetrating peptides), homing peptides, and BBB-shuttles, among others. Some of these new vectors have even reached clinical trials. Consequently, many groups are dedicated to peptide drug design for

anticancer cancer drug delivery and researching new appealing qualities such as resistance to protease degradation (Sanchez-Navarro et al. 2017).

Also for the future, the fusion of nanotechnology, materials science, and biotechnology is bringing progress in the medical technologies used for the diagnosis and treatment of cancer, as well as the monitoring of drug delivery. Lipid-based or organometallic nanoconjugations with anticancer peptides clearly represent new options in the management of this critically important disease. For the success of nanoconjugates, further combinations should be studied and further tests are required to access their viability and bioactivity. Most importantly, the long-term safety of nanomaterials for *in vivo* applications should be confirmed. It is also necessary to devise a means of mass producing nanoparticles, as well as optimizing their dose or concentration, flow rate, size of the microfluidic channel reactor, and so forth.

The decoration of a nanoparticle with CT-p19LC could be of interest for further exploration for the purpose of studying improved drug delivery mechanisms. Given that this peptide appears to be more active against cancer cells instead of non-malignant cells, an efficient system of delivering the peptide near the cancer zone has potential to represent a very safe and proficient type of therapy in the future.

Also, the enhanced effect observed to exist when lung A549 cancer cell treatment included both CT-p19LC and erlotinib provides significant conclusions. Synergy between two drugs means that it is possible to upgrade the toxic effect against cancer cells while diminishing the toxic effect the drugs have on healthy cells, by decreasing their concentration. It is not unheard of that some anticancer peptides have been conjugated with known chemotherapeutic drugs, in smaller doses than normally administered, and proved to be more effective in clinical trials. For instances, the anticancer peptide romidepsin is a FDA approved anticancer agent against T-cell lymphoma when used alone. Although very effective against hematological tumors, its efficacy was always less significant against solid tumors. Currently, the potential action of this peptide against breast cancer in synergy with Abraxene® (paclitaxel albumin-stabilized nanoparticles) is being tested in humans (NCT01938833). Initially developed to avoid the toxicities associated with polyethylated castor oil, the novel neoadjuvant agent Abraxene® have already proved in a serial of clinical trials recently reviewed by Zong et al. to be an effective solo cytotoxic drug in chemotherapy for primary breast cancer patients, especially in aggressive subtypes (Zong et al. 2017).

Consequently, a nanoparticle containing erlotinib could be decorated with CT-p19LC and its efficacy studied in the future, not only regarding potential cytotoxicity against lung cancer but also hopefully providing data regarding their specificity and promoting drug delivery fine-tuning.

Finally, further studies into this emerging field of anticancer peptides need to be embraced. More *in vitro* studies need to be conducted correlating with the effects reported on numerous cancer cell lines. Understanding the detailed and precise mechanisms of this class of agents and structure-activity relationship will provide a knowledge platform to respond to some unanswered questions about both anticancer and antimicrobial peptides which will most possibly allow the design of superior agents. Instability and degradation of the peptides need to be further studied in order for these agents to exert their full therapeutic potentials and perhaps decipher some activities unknown in the present days.

6. References

- Al-Benna, S. et al., 2011. Oncolytic Activities of host defense peptides. *International Journal of Molecular Sciences*, 12(11), pp.8027–8051.
- Al-Hajj, M. & Clarke, M.F., 2004. Self-renewal and solid tumor stem cells. *Oncogene*, 23, pp.7274–7282.
- Allen, J.D. et al., 2002. Potent and specific inhibition of the breast cancer resistance protein multidrug transporter in vitro and in mouse intestine by a novel analogue of fumitremorgin C. *Molecular cancer therapeutics*, 1(6), pp.417–25.
- Ausbacher, D. et al., 2012. Anticancer mechanisms of action of two small amphipathic β 2,2-amino acid derivatives derived from antimicrobial peptides. *Biochimica et Biophysica Acta - Biomembranes*, 1818(11), pp.2917–2925.
- Baxter, A. et al., 2017. Tumor cell membrane-targeting cationic antimicrobial peptides : novel insights into mechanisms of action and therapeutic prospects. *Cellular and Molecular Life Sciences*, (August).
- Bernardes, N. et al., 2014. High-throughput molecular profiling of a P-cadherin overexpressing breast cancer model reveals new targets for the anti-cancer bacterial protein azurin. *International Journal of Biochemistry and Cell Biology*, 50, pp.1–9.
- Bernardes, N. et al., 2016. Modulation of membrane properties of lung cancer cells by azurin enhances the sensitivity to EGFR-targeted therapy and decreased β 1 integrin-mediated adhesion. *Cell Cycle*, 15(11), pp.1415–1424.
- Boohaker, R.J. et al., 2015. The Use of Therapeutic Peptides to Target and to Kill Cancer Cells. *HHS Public Access*, 19(22), pp.3794–3804.
- Bradford, M.M., 1976. A Rapid and Sensitive Method for the Quantitation Microgram Quantities of Protein Utilizing the Principle of Protein-Dye Binding. *Analytical Biochemistry*, 72(2), pp.248–254.
- Calabrese, E.J., 2004. Hormesis: a revolution in toxicology, risk assessment and medicine. *science & society*, 5, pp.37–40.
- Chakrabarty, A.M., Bernardes, N. & Fialho, A.M., 2014. Bacterial proteins and peptides in cancer therapy. *Bioengineered*, 5(4), pp.234–242.
- Chaudhari, A. et al., 2007. Cupredoxin - Cancer Interrelationship: Azurin Binding with EphB2 , Interference in EphB2 Tyrosine Phosphorylation , and Inhibition of Cancer Growth. *Biochemistry*, (46), pp.1799–1810.
- Chen, C. et al., 2012. Molecular mechanisms of antibacterial and antitumor actions of designed surfactant-like peptides. *Biomaterials*, 33(2), pp.592–603.
- Chen, J.-Y. et al., 2009. Epinecidin-1 peptide induces apoptosis which enhances antitumor effects in human leukemia U937 cells. *Peptides*, 30(12), pp.2365–2373.
- Chen, Y. et al., 2001. RGD-Tachyplesin inhibits tumor growth. *Cancer research*, 61(6), pp.2434–8.
- Chen, Y.C. et al., 2015. Anti-proliferative effect on a colon adenocarcinoma cell line exerted by a membrane disrupting antimicrobial peptide KL15. *Cancer Biology and Therapy*, 16(8), pp.1172–1183.

- Chu, E. & De Vita, V.J., 2015. Principles of cancer chemotherapy. Physicians' cancer chemotherapy drug manual, 2016. , pp.1–4.
- Cohen, A.W. et al., 2004. Role of Caveolae and Caveolins in Health and Disease. *Physiological reviews*, (84), pp.1341–1379.
- Dornan, D., 2006. ATM Engages Autodegradation of the E3 Ubiquitin Ligase COP1 After DNA Damage. *Science*, 313(5790), pp.1122–1126.
- Drain, N. et al., 2009. Human defensins as cancer biomarkers and antitumour molecules. *Journal of Proteomics*, 72(6), pp.918–927.
- Ferlay, J. et al., 2013. Cancer incidence and mortality patterns in Europe: Estimates for 40 countries in 2012. *European Journal of Cancer*, 49(6), pp.1374–1403.
- Fialho, A.M., Bernardes, N. & Chakrabarty, A., 2016. Exploring the anticancer potential of the bacterial protein azurin. *AIMS Microbiology*, 2(3), pp.292–303.
- Fialho, A.M., Bernardes, N. & Chakrabarty, A.M., 2012. Recent patents on live bacteria and their products as potential anticancer agents. *Recent Patents on Anti-Cancer Drug Discovery*, 7, pp.31–55.
- Folkman, J., 1971. Tumor angiogenesis: therapeutic implications. *The New England journal of medicine*, 285(21), pp.1182–1186.
- Gaspar, D. et al., 2015. Apoptotic human neutrophil peptide-1 anti-tumor activity revealed by cellular biomechanics. *BBA - Molecular Cell Research*, 1853(2), pp.308–316.
- Gaspar, D., Salomé Veiga, A. & Castanho, M.A.R.B., 2013. From antimicrobial to anticancer peptides. A review. *Frontiers in Microbiology*, 4(OCT), pp.1–16.
- Gatti, L. & Zunino, F., 2005. Overview of tumor cell chemoresistance mechanisms. *Methods in molecular medicine*, 111, pp.127–148.
- Ghandehari, F. et al., 2015. In silico and in vitro studies of cytotoxic activity of different peptides derived from vesicular stomatitis virus G protein. *Iranian Journal of Basic Medical Sciences*, (18), pp.47–52.
- Gupta, D.T., 2002. Bacterial redox protein azurin, tumor suppressor protein p53, and regression of cancer. *Proc Natl Acad Sci U S A*, (22), pp.14098–103.
- Hamill, S.J. et al., 2000. Conservation of folding and stability within a protein family: the tyrosine corner as an evolutionary cul-de-sac. *Journal of molecular biology*, 295(3), pp.641–9.
- Harris, F. et al., 2011. On the selectivity and efficacy of defense peptides with respect to cancer cells. *Medicinal Research Reviews*, 29(6), pp.1292–1327.
- Hilchie, A.L. et al., 2011. Pleurocidin-family cationic antimicrobial peptides are cytolytic for breast carcinoma cells and prevent growth of tumor xenografts. *Breast Cancer Research*, 13(5), p.R102.
- Hoskin, D.W. & Ramamoorthy, A., 2008. Studies on anticancer activities of antimicrobial peptides. *Biochimica et Biophysica Acta - Biomembranes*, 1778(2), pp.357–375.
- Howe, G.A. et al., 2016. Focal Adhesion Kinase Inhibitors in Combination with Erlotinib Demonstrate Enhanced Anti-Tumor Activity in Non-Small Cell Lung Cancer. *Plos one*, pp.1–20.
- Huang, Z., 2000. Bcl-2 family proteins as targets for anticancer drug design. *Oncogene*, 19(56), pp.6627–

6631.

- Jia, L. et al., 2011. Preclinical pharmacokinetics, metabolism, and toxicity of azurin-p28 (NSC745104) a peptide inhibitor of p53 ubiquitination. *Cancer Chemotherapy and Pharmacology*, 68(2), pp.513–524.
- Karagiannis, E.D. & Popel, A.S., 2008. A systematic methodology for proteome-wide identification of peptides inhibiting the proliferation and migration of endothelial cells. *Proceedings of the National Academy of Sciences of the United States of America*, 105(37), pp.13775–80.
- Kastan, M.B. & Bartek, J., 2004. Cell-cycle checkpoints and cancer. *Nature*, 432(7015), pp.316–323.
- Kaur, S. & Kaur, S., 2015. Bacteriocins as potential anticancer agents. *Frontiers in Pharmacology*, 6(NOV), pp.1–11.
- Kloudova, A., Guengerich, F.P. & Soucek, P., 2017. The Role of Oxysterols in Human Cancer. *Trends in Endocrinology & Metabolism*, 28(7), pp.485–496.
- Koskimaki, J.E. et al., 2009. Peptides derived from type IV collagen, CXC chemokines, and thrombospondin-1 domain-containing proteins inhibit neovascularization and suppress tumor growth in MDA-MB-231 breast cancer xenografts. *Neoplasia (New York, N.Y.)*, 11(12), pp.1285–1291.
- Kumar, S. & Li, H., 2017. In Silico Design of Anticancer Peptides. *Proteomics for Drug Discovery: Methods and Protocols*, 1647.
- Lee, J.H. et al., 2015. Anticancer activity of CopA3 dimer peptide in human gastric cancer cells. *Biochemistry and Molecular Biology*, 48(6), pp.324–329.
- Leuschner, C., 2005. Targeting Breast and Prostate Cancers Through Their Hormone Receptors. *Biology of Reproduction*, 73(5), pp.860–865.
- Li, G. et al., 2014. Tryptophan as a Probe to Study the Anticancer Mechanism of Action and Specificity of α -Helical Anticancer Peptides. *Molecules*, (19), pp.12224–12241.
- Li, Y.C. et al., 2006. Elevated levels of cholesterol-rich lipid rafts in cancer cells are correlated with apoptosis sensitivity induced by cholesterol-depleting agents. *The American journal of pathology*, 168(4), pp.1107–18–5.
- Lin, W.J. et al., 2009. Epinecidin-1, an antimicrobial peptide from fish (*Epinephelus coioides*) which has an antitumor effect like lytic peptides in human fibrosarcoma cells. *Peptides*, 30(2), pp.283–290.
- Liotta, L. a., 1984. Tumor Invasion and Metastases: Role of the Basement Membrane. *American Journal of Pathology*, 117(3), pp.339–348.
- Lowe, S.W. & Lin, A.W., 2000. Apoptosis in cancer. *Carcinogenesis*, 21(3), pp.485–495.
- Lulla, R.R. et al., 2016. Phase i trial of p28 (NSC745104), a non-HDM2-mediated peptide inhibitor of p53 ubiquitination in pediatric patients with recurrent or progressive central nervous system tumors: A Pediatric Brain Tumor Consortium Study. *Neuro-Oncology*, 18(9), pp.1319–1325.
- Ma, J. et al., 2013. Isolation and purification of a peptide from bullacta exarata and its impaction of apoptosis on prostate cancer cell. *Marine Drugs*, 11(1), pp.266–273.
- Mader, J.S. & Hoskin, D.W., 2006. Cationic antimicrobial peptides as novel cytotoxic agents for cancer treatment. *Expert opinion on investigational drugs*, 15(8), pp.933–46.

- Malvezzi, M. et al., 2016. European Cancer Mortality Predictions For The Year 2016. *Annals of Oncology Advance Access*.
- Martinez-outschoorn, U.E., Sotgia, F. & Lisanti, M.P., 2015. Caveolae and signalling in cancer. *Nature Publishing Group*, 15(4), pp.225–237.
- Mohd, K.S. et al., 2015. A review of potential anticancers from antimicrobial peptides. *International Journal of Pharmacy and Pharmaceutical Sciences*, 7(4), pp.19–26.
- Murai, T., 2015. Cholesterol lowering : role in cancer prevention and treatment. *Biological chemistry*, 396(1), pp.1–11.
- Nes, I. & Holo, H., 2000. Class II antimicrobial peptides from lactic acid bacteria. *Peptide Science*, pp.50–61.
- Nguyen, L.T., Haney, E.F. & Vogel, H.J., 2011. The expanding scope of antimicrobial peptide structures and their modes of action. *Trends in Biotechnology*, 29(9), pp.464–472.
- Nichols, M. et al., 2013. Cardiovascular disease in Europe: Epidemiological update. *European Heart Journal*, 34(39), pp.3028–3034.
- Ourth, D.D., 2011. Antitumor cell activity in vitro by myristoylated-peptide. *Biomedicine and Pharmacotherapy*, 65(4), pp.271–274.
- Owen, D.M. et al., 2011. Quantitative imaging of membrane lipid order in cells and organisms. *Nature Protocols*, 7(1), pp.24–35.
- Paiva, A.D. et al., 2012. Toxicity of bovicin HC5 against mammalian cell lines and the role of cholesterol in bacteriocin activity. *Microbiology*, (158), pp.2851–2858.
- Pang, H., Le, P.U. & Nabi, I.R., 2004. Ganglioside GM1 levels are a determinant of the extent of caveolae / raft-dependent endocytosis of cholera toxin to the Golgi apparatus. *Journal of Cell Science*, (117), pp.1421–1430.
- Papo, N. et al., 2006. Inhibition of tumor growth and elimination of multiple metastases in human prostate and breast xenografts by systemic inoculation of a host defense-like lytic peptide. *Cancer Research*, 66(10), pp.5371–5378.
- Patel, S. & Player, M.R., 2008. Small-molecule inhibitors of the p53-HDM2 interaction for the treatment of cancer. *Expert opinion on investigational drugs*, 17(12), pp.1865–82.
- Pinto, S.N. et al., 2013. A combined fluorescence spectroscopy , confocal and 2-photon microscopy approach to re-evaluate the properties of sphingolipid domains. *BBA - Biomembranes*, 1828(9), pp.2099–2110.
- Preet, S. et al., 2015. Effect of nisin and doxorubicin on DMBA-induced skin carcinogenesis — a possible adjunct therapy. *Tumor Biology*.
- Proskuryakov, S.Y. & Gabai, V.L., 2010. Mechanisms of tumor cell necrosis. *Current pharmaceutical design*, 16(1), pp.56–68.
- Punj, V. et al., 2004. Bacterial cupredoxin azurin as an inducer of apoptosis and regression in human breast cancer. *Oncogene*, 23(13), pp.2367–78.
- Purcell, A.W., McCluskey, J. & Rossjohn, J., 2007. More than one reason to rethink the use of peptides in

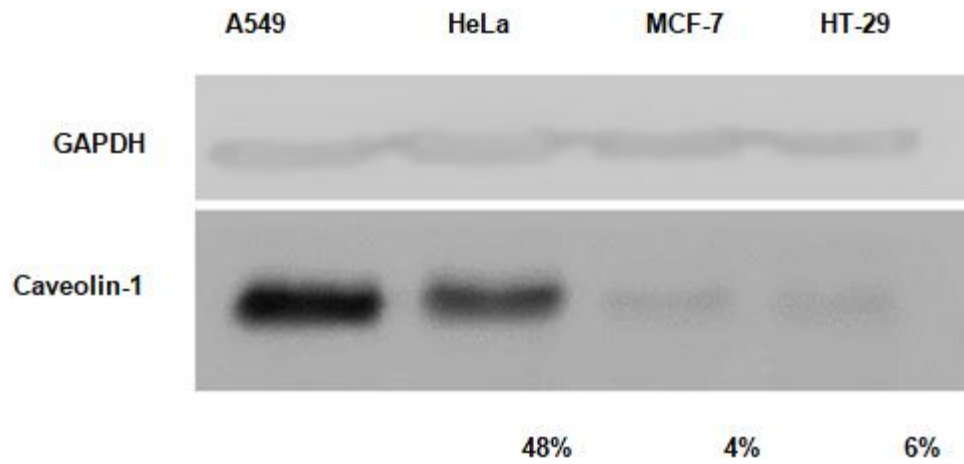
- vaccine design. *Nature reviews. Drug discovery*, 6(5), pp.404–414.
- Quest, A.F.G., Gutierrez-pajares, J.L. & Torres, V.A., 2008. An ambiguous partner in cell signalling and cancer The caveolins. *Journal of Cellular and Molecular Medicine*, 12(4), pp.1130–1150.
- Reynolds, A.R., 2010. Potential relevance of bell-shaped and u-shaped dose-responses for the therapeutic targeting of angiogenesis in cancer. *Dose-Response*, 8(3), pp.253–284.
- Riedl, S., Zweytick, D. & Lohner, K., 2011. Membrane-active host defense peptides - Challenges and perspectives for the development of novel anticancer drugs. *Chemistry and Physics of Lipids*, 164(8), pp.766–781.
- Rodrigues, E.G. et al., 2009. Antifungal and antitumor models of bioactive protective peptides. *Anais da Academia Brasileira de Ciencias*, 81(3), pp.503–520.
- Rothberg, K.G. et al., 1992. Caveolin , a Protein Component of Caveolae Membrane Coats. *Cell*, 68, pp.673–682.
- Sanchez-Navarro, M., Teixido, M. & Giralt, E., 2017. Jumping Hurdles: Peptides Able To Overcome Biological Barriers. *Accounts of Chemical Research*, (50), pp.1847–1854.
- Sanchez, S.A. et al., 2011. Methyl- β -Cyclodextrins Preferentially Remove Cholesterol from the Liquid Disordered Phase in Giant Unilamellar Vesicles. *Journal of Membrane Biology*, (241), pp.1–10.
- Siegel, R., Miller, K. & Jemal, A., 2015. Cancer statistics , 2015 . *CA Cancer J Clin*, 65(1), p.29.
- Singh, R.D. et al., 2003. Selective Caveolin-1 – dependent Endocytosis of Glycosphingolipids. *Molecular Biology of the Cell*, 14(August), pp.3254–3265.
- Sinthuvanich, C. et al., 2011. Anticancer β -Hairpin Peptides: Membrane-Induced Folding Triggers Activity. *Journal of the American Chemical Society*, (134), pp.6210–6217.
- Srisailam, S. et al., 2001. Crumpled structure of the custom hydrophobic lytic peptide cecropin B3. *European Journal of Biochemistry*, (268), pp.4278–4284.
- Tannishtha, R. et al., 2001. Stem cells, cancer, and cancer stem cells. *Nature*, 414(November), pp.105–111.
- Taylor, B.N. et al., 2009. Noncationic peptides obtained from azurin preferentially enter cancer cells. *Cancer Research*, 69(2), pp.537–546.
- Teixeira, V., Feio, M.J. & Bastos, M., 2012. Role of lipids in the interaction of antimicrobial peptides with membranes. *Progress in Lipid Research*, 51(2), pp.149–177.
- Torre, L.A. et al., 2015. Global Cancer Statistics, 2012. *CA: a cancer journal of clinicians.*, 65(2), pp.87–108.
- Tyagi, A. et al., 2013. In silico models for designing and discovering novel anticancer peptides. *Scientific reports*, 3, p.2984.
- VanderMolen, K.M. et al., 2011. Romidepsin (Istodax, NSC 630176, FR901228, FK228, depsipeptide): a natural product recently approved for cutaneous T-cell lymphoma. *The Journal of antibiotics*, 64(8), pp.525–31.
- Wang, C. et al., 2013. Anticancer mechanisms of temporin-1CEa, an amphipathic α -helical antimicrobial

- peptide, in Bcap-37 human breast cancer cells. *Life Sciences*, 92(20–21), pp.1004–1014.
- Wang, G., Li, X. & Wang, Z., 2009. APD2: The updated antimicrobial peptide database and its application in peptide design. *Nucleic Acids Research*, 37(SUPPL. 1), pp.933–937.
- Wang, K. et al., 2008. Antitumor effects, cell selectivity and structure-activity relationship of a novel antimicrobial peptide polybia-MPI. *Peptides*, 29(6), pp.963–968.
- Wang, Y.S. et al., 2009. Intratumoral expression of mature human neutrophil peptide-1 mediates antitumor immunity in mice. *Clinical Cancer Research*, 15(22), pp.6901–6911.
- Warso, M.A. et al., 2013. A first-in-class, first-in-human, phase I trial of p28, a non-HDM2-mediated peptide inhibitor of p53 ubiquitination in patients with advanced solid tumours. *British journal of cancer*, 108(5), pp.1061–70.
- WHO, 2015. *The World Cancer Report*, Geneva.
- Williams, T.M. et al., 2004. Caveolin-1 Gene Disruption Promotes Mammary Tumorigenesis and Dramatically Enhances Lung Metastasis in Vivo. *The Journal Of Biological Chemistry*, 279(49), pp.51630–51646.
- Wong, D.Y.Q., Lim, J.H. & Ang, W.H., 2015. Induction of targeted necrosis with HER2-targeted platinum(IV) anticancer prodrugs. *Chem. Sci.*, 6, pp.3051–3056.
- Xu, H. et al., 2013. Dual modes of antitumor action of an amphiphilic peptide A9K. *Biomaterials*, 34(11), pp.2731–2737.
- Yamada, T. et al., 2009. A peptide fragment of azurin induces a p53-mediated cell cycle arrest in human breast cancer cells. *Molecular cancer therapeutics*, 8(10), pp.2947–58.
- Yamada, T. et al., 2016. *p28-mediated Activation of p53 in G2/M Phase of the Cell Cycle Enhances the Efficacy of DNA Damaging and Antimitotic Chemotherapy*,
- Yamada, T. et al., 2013. p28, A first in class peptide inhibitor of cop1 binding to p53. *British Journal of Cancer*, 108(12), pp.2495–2504.
- Yamada, T. et al., 2004. Regulation of Mammalian Cell Growth and Death Relevance by Bacterial Redox Proteins. *Cell Cycle*, 3(June), pp.752–755.
- Yang, W. et al., 2008. TMTP1, a novel tumor-homing peptide specifically targeting metastasis. *Clinical Cancer Research*, 14(17), pp.5494–5502.
- Yang, Z. et al., 2017. Comparison of gefitinib, erlotinib and afatinib in non-small cell lung cancer: a meta-analysis. *Cancer Therapy and Prevention*, pp.1–39.
- Zaslhoff, M., 2002. Antimicrobial peptides of multicellular organisms. *Nature*, 415(0028–0836 (Print)), pp.389–395.
- Zong, Y., Wu, J. & Shen, K., 2017. Nanoparticle albumin-bound paclitaxel as neoadjuvant chemotherapy of breast cancer: a systematic review and meta-analysis. *Oncotarget*.

Appendix

Table_S1| Representation of *in silico* study on similarity between CT-p26 azurin's region in various *Pseudomonas aeruginosa* strains where it was concluded that this region is completely conserved within the species.

AU23529	VTFDVSKLKEGEQYMFFCTFPGHSAL
AU24807	
AU17965	
AU14820	
AU10756	
ATCC 33988	
ET02	
Pa538	
PAO1	
PAO1-VE13	
PAO1-VE2	
PAO581	
PA1RG	
PAG	
RNS_PA46	



Figure_S1 | Caveolin-1 levels are different in four adenocarcinoma cell lines. A549, HeLa, MCF-7 and HT-29 human cancer cell lines were grown overnight in 6-well plates with 5×10^5 cells/well. A549 lung cells are the richest in caveolin-1 and in comparison HeLa has less than half of A549 cells' caveolin-1 content and MCF-7 and HT-29 cells' caveolin-1 content are less than 10%. The protein levels were normalized by the respective GAPDH level.

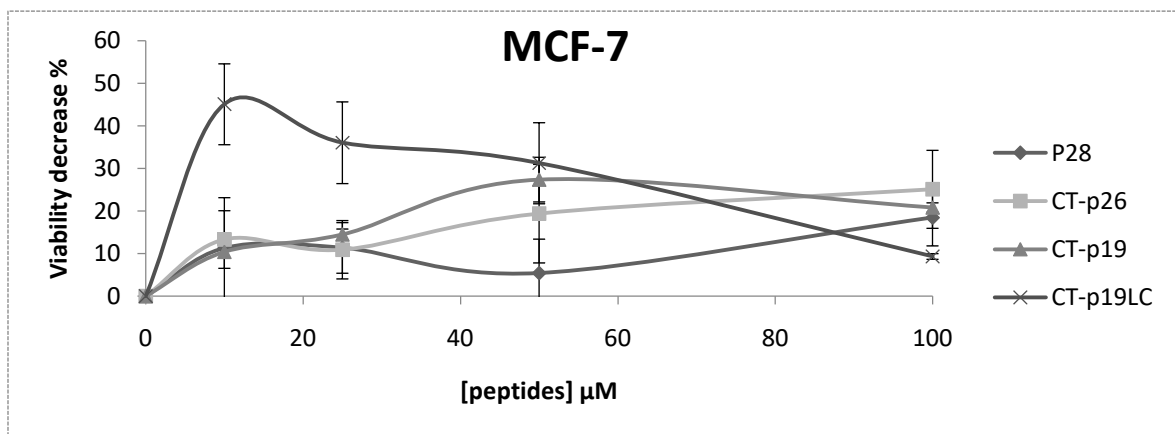
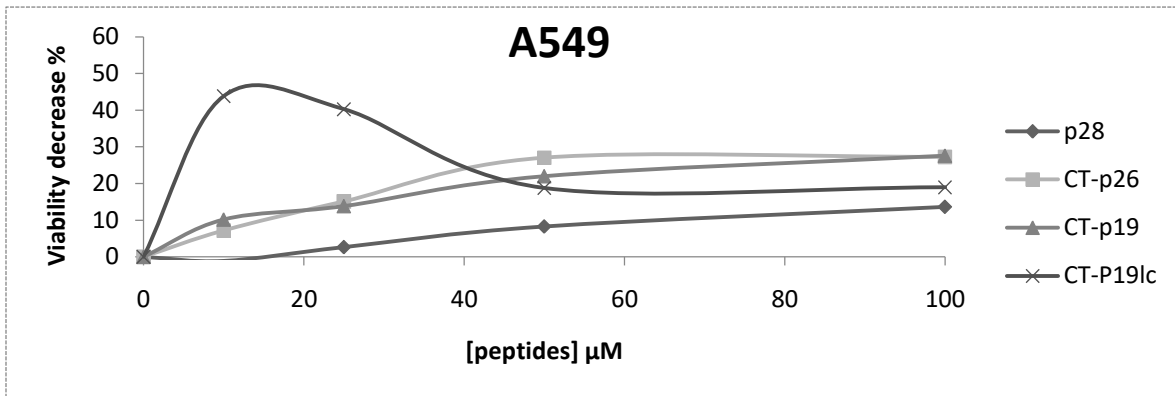
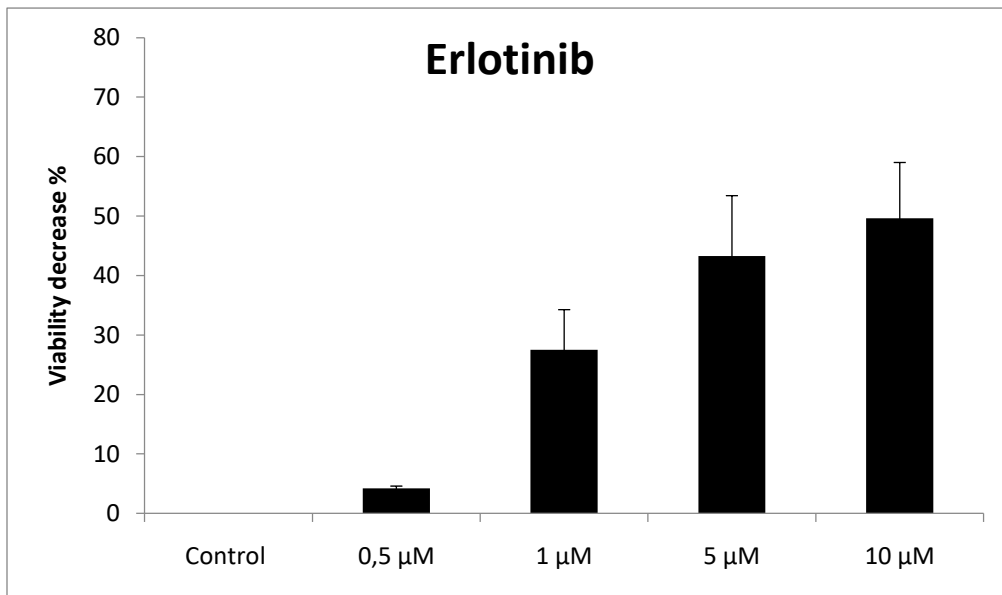


Figure S2 Results from MTT proliferation assay performed on lung A549 cancer cell line (above) and breast MCF-7 cancer cell line (bellow) upon treatment with p28, CT-p26, CT-p19 and CT-p19LC in concentrations of 10, 25, 50 and 100 μM , for 48h.



Figure_S3| The effects of erlotinib treatment on A549 human cancer cell line. All these cell lines were seeded overnight in 96-well plates (3 replicates) with a density of 4×10^3 cells per well. Following, these cells were treated with 0,5 1, 5 and 10 μM of erlotinib during 72 hours. Untreated cells were used as control.